Journal of Energy Chemistry 25 (2016) 208–224

Contents lists available at ScienceDirect

Journal of Energy Chemistry

journal homepage: www.elsevier.com/locate/jechem

http://www.journals.elsevier.com/journal-of-energy-chemistry/

Review

Transformation of bio-derived acids into fuel-like alkanes via ketonic decarboxylation and hydrodeoxygenation: Design of multifunctional catalyst, kinetic and mechanistic aspects

Irina L. Simakova[a,b], Dmitry Yu. Murzin[c,*]

[a] Boreskov Institute of Catalysis, Novosibirsk 630090, Russian Federation
[b] Novosibirsk State University, Novosibirsk 630090, Russian Federation
[c] Åbo Akademi University, Turku FI-20500, Finland

ARTICLE INFO

Article history:
Received 9 November 2015
Revised 8 December 2015
Accepted 10 December 2015
Available online 13 January 2016

Keywords:
Carboxylic acids
Ketonization
Hydrodeoxygenation
Alkane
Biofuel

ABSTRACT

The combination of a low cost source of Biofine's levulinic acid with available way of valeric acid synthesis opens up new opportunities for valeric acid as a promising bio-derived source for synthesis of valuable compounds for transportation sector. The present review illustrates the development of different approaches to one–pot synthesis of fuel-like alkanes from lignocellulose derived carboxylic acids where particular focus is given to valeric acid consecutive decarboxylative coupling (ketonization) and ketone hydrodeoxygenation in a single reactor over one catalyst bed. The key factors that influence the catalytic performance on both ketonization and hydrodeoxygenation steps as well as their cross-influence will be clarified to provide insights for the design of more efficient catalysts for the one-pot transformation. Valeric acid is considered as a potential acid source from viewpoint of cost effectiveness and feasibility of such transformation with reasonable alkane yield. The both reaction mechanisms and kinetics will also be discussed to understand deeply how the selective C–C coupling and following C=O hydrogenation can be achieved.

1. Introduction

The biomass-based technologies have been acknowledged as becoming competitive options to convert bioresources into fuels/chemicals having the potential to replace at least a certain parts of the total fossil fuel consumption. The interest in biomass conversion to value-added chemicals increased constantly during the last 10 years in industry and academia. For the former it is a challenge to find alternative syntheses for substances that are currently obtained starting from petroleum. The challenge that might also be a chance is that bio-derived and petroleum-based feedstock involve diametrically opposite polarity characteristics. Petroleum consists of apolar hydrocarbons, immiscible with water, that have to be oxy-functionalized in many cases in industrial processes when chemicals rather than fuels are desired. On the contrary, biomass consists of highly oxy-functionalized molecules that have to be dehydrated and hydrogenated, especially if alkane-based fuels are the desired products [1,2]. In the transformation of lignocellulosic biomass into fuels and chemicals carbon–carbon bond formations and increasing hydrophobicity are highly desired. Ketonic decarboxylation fits these requirements very well as in this reaction carboxylic acids are converted into ketones forming one carbon–carbon bond and eliminates three oxygen atoms as carbon dioxide and water. This reaction could be used in a cascade mode together with hydrogenation and dehydration catalysts to obtain hydrocarbons in the kerosene range from hexose-derived valeric acid (VA) [3]. In the case of chemicals alternative ways of synthesis are possible which might even be more economical when an advantage is taken from the molecule structure. This progress has to be supported by academia by developing and optimizing synthesis methods that accept biomass platform molecules as starting materials. Cost effective processes adapted to the molecular structure of highly functionalized biomass molecules have to be designed to make the quality and price of chemical compounds more competitive with respect to those obtained by traditional routes. A number of publications dedicated to biomass conversion into fuel and chemicals increased dramatically during the last years [4–9]. Extensive literature surveys covering this subject were published recently [10–17].

The present review illustrates one of the promising approaches for the synthesis of fuel-like alkanes from lignocellulose derived acids including consecutive decarboxylative coupling (ketonization)

---

* Corresponding author. Tel: +358 2 215 4985; Fax: +358 2 215 4479.
E-mail address: dmurzin@abo.fi (D.Yu. Murzin).

http://dx.doi.org/10.1016/j.jechem.2016.01.004
2095-4956/

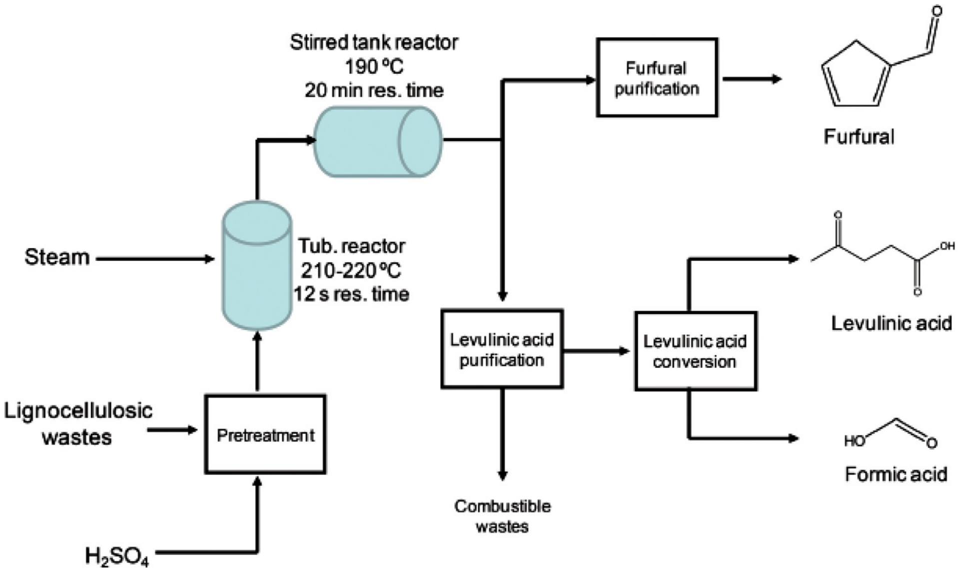

Fig. 1. Scheme of the Biofine process developed for the conversion of lignocellulosic wastes into levulinic acid [30]. Reproduced with permission from Royal Society of Chemistry.

and ketone hydrogenation in a single reactor. Valeric acid is viewed as a potential acid source for this process taking into account cost effectiveness and feasibility of such transformation through different ways with a reasonable alkane yield.

2. Alkanoic acids as a cost effective starting material

An interesting trend in current biomass conversion strategies involves utilization of biomass-derived alkanoic acids coming from cellulose, hemicellulose, tall oil and vegetable oil for production of valuable chemicals and motor fuel components [18–24]. Levulinic acid being one of important bio-derived platform molecules plays a predominant role in biomass transformations into fuels and chemicals when lignocellulose is considered as a raw material [25].

2.1. Synthesis of levulinic acid

Levulinic acid has been known as a versatile chemical for over 50 years, however earlier levulinic acid (LA, 4-oxopentanoic acid) has been often considered as an expensive and relatively small market specialty chemical (with about 1 million lb/year production at a selling price \$4.00–\$6.00/lb) [26–28]. Such high price has inhibited its widespread use, however, recent economic projections indicated that the LA production cost could fall as low as \$0.04–\$0.10/lb depending on the scale of the operation due to a new LA production process developed by Biofine Corporation [2,29,30] (Fig. 1). The technology has been demonstrated on a 1 ton/day scale at a facility in South Glens Falls, New York.

2.2. Synthesis of valeric acid

This cost effective production allows LA to be an economic starting material for production of fuel substitutes, monomers, novel pesticides and a wide range of commodity chemicals, such as γ-valerolactone (GVL), valeric acid (VA) and their derivatives. VA can be prepared from LA either through a single-step or two-stage process going first through GVL synthesis and its further conversion to VA. Kon et al. [31] were the first to report a highly selective single-step conversion of LA to VA or valeric acid esters over Pt/HMFI catalyst under low H_2 pressure (0.2 or 0.8 MPa) conditions, with selectivity to VA or its esters being completely dependent on the solvent used. The reaction starts with hydrogenation on Pt sites of LA to GVL, which undergoes ring-opening on Bronsted acid sites of H-MFI to give pentenoic acid. This intermediate is hydrogenated on Pt sites to yield VA. If the ring-opening Bronsted acid sites are not near the hydrogenation sites (Pt), pentenoic acid as an intermediate could undergo polymerization. This is a possible reason why a physical mixture of Pt/SiO_2 and HMFI gives a lower yield (~48%) than Pt/HMFI (~83% in toluene, 99% in solvent-free conditions and 19% in dioxane). Luo et al. also showed [32] that VA can be prepared directly by conversion of LA over 1 wt% Ru/H-ZSM5 at 4 MPa H_2 and 473 K in dioxane with the yield of 91.3% after 10 h (Fig. 2). Direct synthesis, however, suffers from catalyst deactivation caused by carbon residue deposition on the strong acid sites. Thus a more effective way of VA synthesis includes two separately implemented transformations: first LA conversion to GVL followed by conversion of the latter into VA.

Different approaches to GVL synthesis from LA have been reported. The review [6] pinpointed the unique physical and chemical properties of GVL which makes it an ideal liquid for use as an intermediate in chemical industry or for energy storage [33].

As discussed in [6] GVL was obtained with 97% yield by hydrogenation of levulinic acid at 423 K over 5 wt% Ru/C catalyst. Hydrogenation was optimized by making a continuous process over Ru/SiO_2 catalyst in supercritical CO_2 resulting in 99% yield and an easy separation of GVL from water [6]. Pt/TiO_2 or Pt/ZrO_2 catalysts afforded continuous hydrogenation of levulinic acid with marginal deactivation over 100 h yielding 95% of GVL [6]. The direct synthesis of GVL from fructose aqueous solutions without isolation of levulinic acid was achieved with a 62% yield in an autoclave pressurized with hydrogen and loaded with water, trifluoroacetic acid and Ru/C catalyst [6]. Hydrogenation of levulinic acid to GVL was also performed using formic acid as a hydrogen donor in the presence of ruthenium catalysts [34]. Leitner and coworkers [35] conducted hydrogenation of levulinic acid in the presence of ruthenium complexes. Further improvement was achieved over Ni catalysts without any solvent, whereby the GVL yield increased to 92% at 100% levulinic acid conversion [36]. In the second stage of VA synthesis GVL could be effectively converted to VA by combining ring-opening over acid sites and hydrogenation reactions on metal sites (Fig. 3) using a water stable bifunctional Pd/Nb_2O_5 catalyst at moderate temperatures and pressures [37] as well as a variety of other bifunctional metal–acid catalysts (Fig. 3) [38].

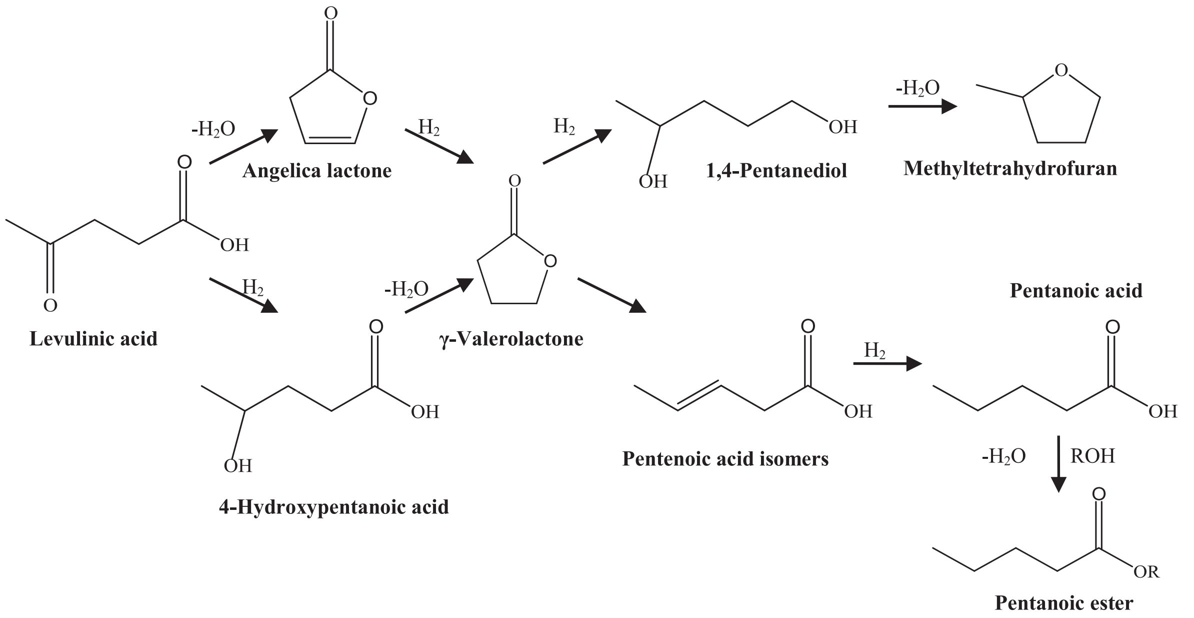

Fig. 2. Scheme of direct LA into VA synthesis over multifunctional Ru/H-ZSM5 [32].

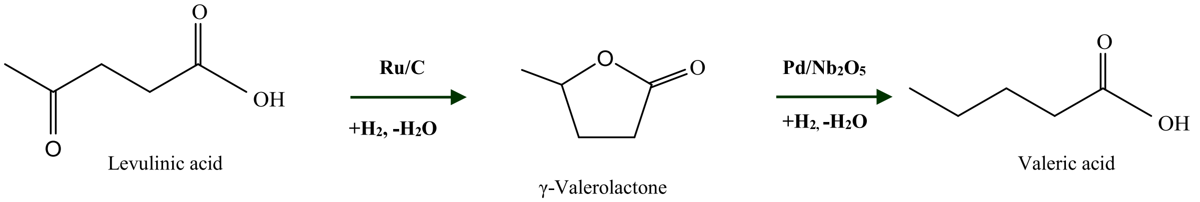

Fig. 3. Scheme of two-step levulinic acid transformation into valeric acid.

Production of the desired VA is, however, accompanied with the formation of *n*-butane by decarboxylation of VA over metal sites with the release of stoichiometric amounts of CO_x, along with *n*-pentane as a result of successive hydrogenations and dehydrations of VA over metal and acid sites, respectively [39].

Importantly, because of its low solubility in water, VA can be obtained in the separator at the effluent of the reactor as an organic layer that is spontaneously separated from water and accumulate almost 80% of the reacted carbon. A decrease in the hydrogen partial pressure in the reactor also favored formation of VA at the expense of hydrogenation and decarboxylation products. A proper choice of the metal catalyst and reaction conditions leads to a yield of VA equal to 92%, with 95% of the carbon being stored in the organic layer (Pd (0.1%)/Nb_2O_5, 50 wt% GVL, 598 K, 3.5 MPa H_2, WHSV = 1.2 h^{-1}) [37]. Overall the two-stage process enables production of VA from levulinic acid with more than 80% yield. Combination of a low cost source of Biofine's LA with a chemically and technologically feasible way of VA synthesis will help to explore new opportunities of VA utilization as a promising bio-derived source for further synthesis of added-value compounds.

3. Promising strategies for synthesis of fuel-like alkanes from carboxylic acids

Synthesis of alkanes from carboxylic acids is of great interest, thus a substantial effort was put on establishing processes that transform different biomass-derived products into liquid fuels and chemicals. The main strategies for these transformations considered in the literature involve coupling of carboxylic acids into high molecular weight compounds followed by hydrodeoxygenation to alkanes [40,41] (Fig. 4).

Corma et al. showed a possibility of obtaining good yields of kerosene from VA in a two-bed continuous reactor by combining ZrO_2 and Pt/Al_2O_3 in the presence of hydrogen [3]. The composite catalyst was stable under reaction conditions (Fig. 5). Acid-enriched organic phase obtained after aqueous phase reforming also can be used for such transformation [42]. Branched alkanes for gasoline application were suggested to be prepared through aldol condensation of ketones prior to their hydrogenation to alkanes or post-isomerization of alkanes.

Gurbuz et al. [43] suggested upgrading mono-functional intermediates produced by catalytic conversion of sugars and polyols over Pt–Re/C catalysts (consisting of alcohols, ketones, carboxylic acids, and heterocyclic compounds) to fuel-grade compounds using two catalytic reactors operated in a cascade mode (Fig. 6). The first reactor achieves C–C coupling of monofunctional intermediates using a dual-bed catalytic system, where the upstream catalyst bed $CeZrO_x$ is employed to carry out ketonization of carboxylic acids, and the downstream catalyst bed Pd/ZrO_2 is used to achieve aldol condensation/hydrogenation of alcohols and ketones. It was found that ketonization must be performed prior to aldol condensation/hydrogenation, because the active basic sites in the aldol condensation catalyst are poisoned by the presence of carboxylic acids [42,44]. The high molecular weight ketones produced by C–C coupling reactions in the dual-bed catalyst system are subsequently converted to alkanes by hydrodeoxygenation (i.e., dehydration/hydrogenation) over a Pt/SiO_2–Al_2O_3 catalyst. Using the aforementioned approach, an aqueous feed containing 60 wt% sorbitol was converted to a liquid stream of alkanes, 53% of which consisted of C_{7+} alkanes with minimal branching, desirable for diesel fuel [43].

Hydrocabon-based gasoline or diesel components were reported to be prepared directly from levulinic acid through its

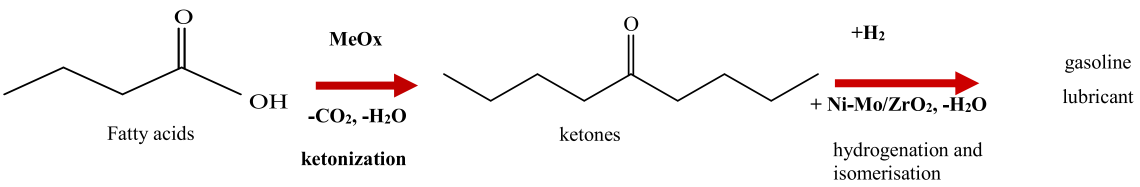

Fig. 4. Scheme of carboxylic acids coupling into high molecular weight compounds followed by hydrodeoxygenation to alkanes [40,41].

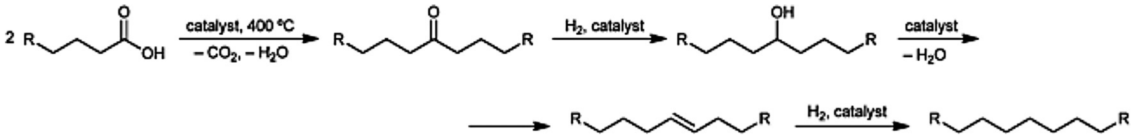

Fig. 5. Reaction sequence involving ketonic decarboxylation, hydrogenation of the resulting ketone to an alcohol, dehydration of the latter, and hydrogenation of the intermediary olefin. For R = *n*-octyl see [40]; R = Me [3].

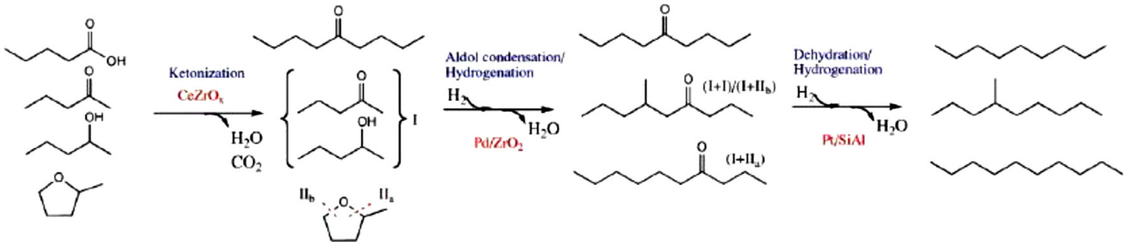

Fig. 6. Reaction pathways for ketonization, aldol condensation/hydrogenation and dehydration/hydrogenation for representative C_5 species. Species IIa and IIb are formed by ring-opening through C–O bond cleavages denoted in the figure [43]. Reproduced with permission from Royal Society of Chemistry.

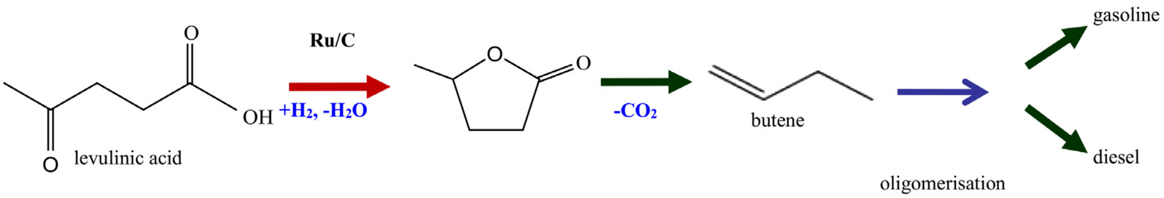

Fig. 7. Direct synthesis of fuel components from levulinic acid [45,46].

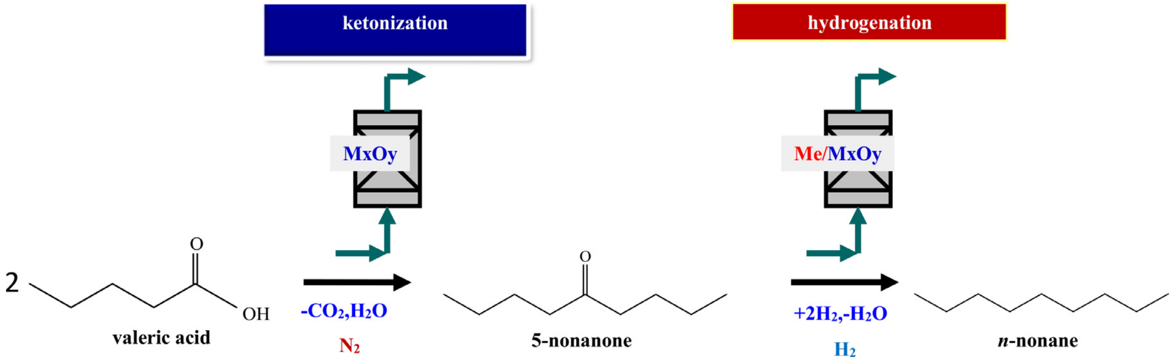

Fig. 8. Scheme of consecutive ketonic decarboxylation and hydrodeoxygenation of valeric acid.

conversion into butene followed by oligomerization to the compounds with a proper mass [45,46] (Fig. 7).

A simple catalytic process to obtain fuels rich in branched alkanes with 8–12 carbons and aromatics via hydrodeoxygenation of biomass-derived angelica lactone dimers/trimers obtained by C–C coupling of α- and β-angelica lactones was investigated [47].

Along with these described strategies catalytic VA transformation into C_9 alkane can be suggested where VA can be converted to the potential fuel components sequentially passing throughout two single-bed reactors: (1) ketonization over a metal oxide in inert atmosphere with CO_2 and H_2O release and (2) hydrodeoxygenation over a platinum group metal with H_2O elimination (Fig. 8). It is worth to note that ketonization itself is a valuable way to upgrade pyrolized bio-oil lowering the acidity, volatility and oxygen content through removal of three oxygen atoms per two acid molecules as carbon dioxide and water.

Realization of this synthesis in one-pot mode is expected to improve the catalytic process through a more efficient interaction of key intermediates on the catalyst surface [3]. Simultaneous ketonization/hydrodeoxygenation also provides better selectivity to linear alkanes due to suppression of a side reaction – aldol condensation [42]. Simakova and coworkers [48] suggested an

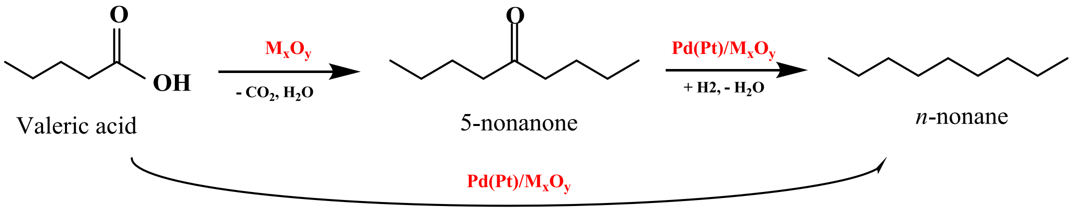

Fig. 9. One-pot synthesis of *n*-nonane from valeric acid on single-bed of bifunctional catalysts in a single reactor after [48].

implementation of this method in a single reactor under hydrogen atmosphere using a single-bed catalytic process in the presence of Pd or Pt supported over active in ketonization reaction metal oxides (Fig. 9). The authors pointed anticipated drawbacks of the one-pot synthesis which they elucidated via a systematical study, such as (i) ketonization should be done in hydrogen instead of a inert gas; (ii) there could be a negative cross-influence of by-products generated during ketonization such as CO_2 and water onto hydrodeoxygenation; and (iii) conditions in the one-pot process can be different from optimal operating conditions for separate reactions.

A major issue is to develop multifunctional catalysts such as multi-site solid catalysts which could be used in cascade-type reactions allowing process intensification. Various challenges in the design of solid catalysts for biomass conversion were reported in the literature [49–51]. Robust and easily regenerated bifunctional catalysts should be developed because side reaction components could alter catalyst selectivity and decrease their activity thus hampering catalyst performance.

This mini-review showcases the challenges in the one-pot transformation of bio-derived C_5 acid into C_9 alkane over a multifunctional catalyst. To design robust bifunctional heterogeneous catalyst, two catalytic reactions were investigated as separate reactions: (i) ketonization over MeO_x in the presence of nitrogen and hydrogen, (ii) hydrogenation of C_9 ketone to C_9 alkane over Pd or Pt on MeO_x in the presence of CO_2 and steam or without them. Finally a optimal catalyst and reaction conditions were examined for one-pot transformation of C_5 acid into C_9 alkane in H_2 atmosphere as well as effectiveness of *n*-nonane synthesis in one-pot vs. two-stage was compared.

4. Carboxylic acid ketonization over MeO_x

One of the promising ways to prepare high molecular weight compounds from short bio-derived carboxylic acids is decarboxylative coupling of acids with formation of ketones. Such ketonization of various carboxylic acids on different metal oxides has been studied extensively, even if the most suitable one has not been identified. Different aspects of acid ketonization were studied to elucidate main regularities and a plausible mechanism for the ketonization reaction [52–54].

4.1. Effect of carboxylic acid structure

Nagashima et al. showed that reactivity of the carboxylic acids was slightly decreased as its chain length increased. In contrast to linear aliphatic acids, branched acids were less reactive. Methyl group substituents at the α- and β-positions of carboxylic acids decreased their reactivities in both homo- and cross-ketonization [52].

4.2. Activity of MeO_x and intermediates formed in ketonization

Glinski et al. first investigated systematically activity of simple mono- and bimetallic oxides (Ag, Bi, Cd, Cu, In, Pb, Re, Cr, Mg, Zn, Ca, Ga, Sr, Ba, Al, Eu, Gd, V, Co, Fe, La, Mn, Zr, Ce, Th and U) deposited on the surface of inorganic supports in the ketonization of propanoic acid into 3-pentanone under the same conditions [55]. It was clearly shown that the studied oxides can be divided into three groups: slightly active, fairly active and highly active. The last group consists of catalysts containing oxides of manganese, zirconium, cerium, thorium, and uranium. No synergistic effect was noted between these oxides. Published reports are mainly focused on the ketonization of aliphatic acids [56–58,67,88], oxy-acids [8,37,59], fatty acids [40,57,60–66,88,101] and dibasic acids [67–69] to form symmetric, non-symmetric, fatty and cyclic ketones over catalysts based on MgO [40,58,101], Nb_2O_5 [8,37,59], CeO_2 [8,52,56,58,70,71,84], MnO_2 [56,58,72,73], TiO_2 [53,56,58,74,97], SiO_2 [56,84], Al_2O_3 [56,58,61,84], ZrO_2 [8,57,58,63,75,76,84,93,94,99], Cr_2O_3 [77,78], Fe_3O_4 [79,80], $Ba(OH)_2$ [67–69], NaOH [81], $FeSO_4$ [67] at 558–723 K, ambient pressure and inert atmosphere. Nevertheless, there are scarce publications concerning influence of a gas flow composition on the oxide catalyst reactivity. Thus Taimoor et al. have reported a beneficial effect of hydrogen on acetic acid conversion in decarboxylative coupling compared with nitrogen and carbon dioxide atmosphere [82] although possible reasons for such changes in catalytic activity were not elucidated.

The acidic character of the reactant imposes specific restrictions on metal oxides in light of their resistance to acidic medium under operation conditions. Thus among Nb_2O_5, CeO_2, ZrO_2, TiO_2, Al_2O_3, MgO catalysts, commonly reported for acid ketonization, MgO was completely dissolved in VA at 90 °C in 3 h, N_2O_5 and CeO_2 lost 6.0 and 3.4% of their initial weight whereas ZrO_2, TiO_2, and Al_2O_3 were unchanged. Lee et al. reported that according to ICP–AES during hexanoic acid ketonization MgO and MnO_x contrary to zirconia were completely dissolved in the liquid products [58]. The results indicated that MgO, MnO_x, CeO_2 and N_2O_5 are not appropriate oxides for supporting noble metals.

In the course of ketonization formation of various intermediates is assumed. Although acid anhydride can be an intermediate during ketonization, mechanisms involving such intermediates explain only decarboxylative cyclization of dicarboxylic acids [83]. The dehydration of dicarboxylic acid starts from anhydride formation with the subsequent decarboxylation and formation of a cyclic ketone. The route through β-ketoacid has been proposed for carboxylic acids with α-hydrogen [83–85]. Such α-hydrogen abstraction of an adsorbed carboxylate results in anion formation, which then reacts with a neighboring carboxylate or acyl to produce β-ketoacid. The ketone is formed by decarboxylation of this intermediate. A concerted mechanism, involving carbon–carbon bond formation and carbon dioxide formation in the same step, explains ketonization of carboxylic acids without α-hydrogen [84,86]. The reaction occurs between two carboxylates or carboxylate and a weakly adsorbed acid molecule.

4.3. Ketonization of valeric acid into 5-nonanone

Only a few publications describe preparation of 5-nonanone by decarboxylative coupling of VA which can be performed in the

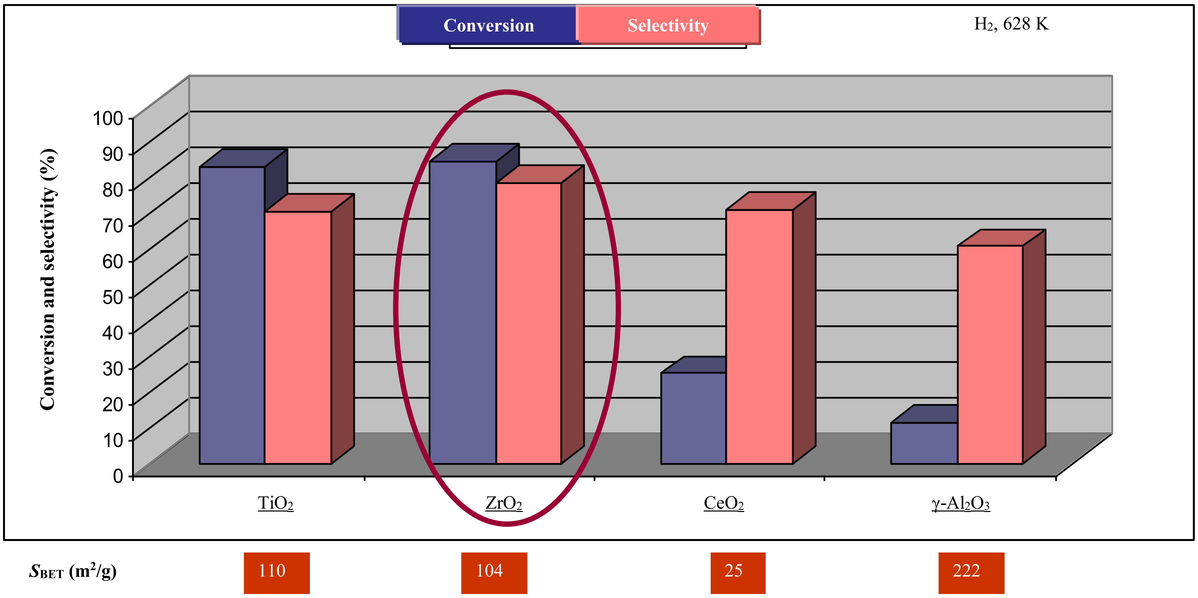

Fig. 10. Catalytic properties of monometallic oxides in valeric acid ketonization. Reaction conditions: C_o (VA) = 4.2 vol%, 628 K, PH_2 = 0.1 MPa, τ = 0.7 s, m_{cat} = 1 g.

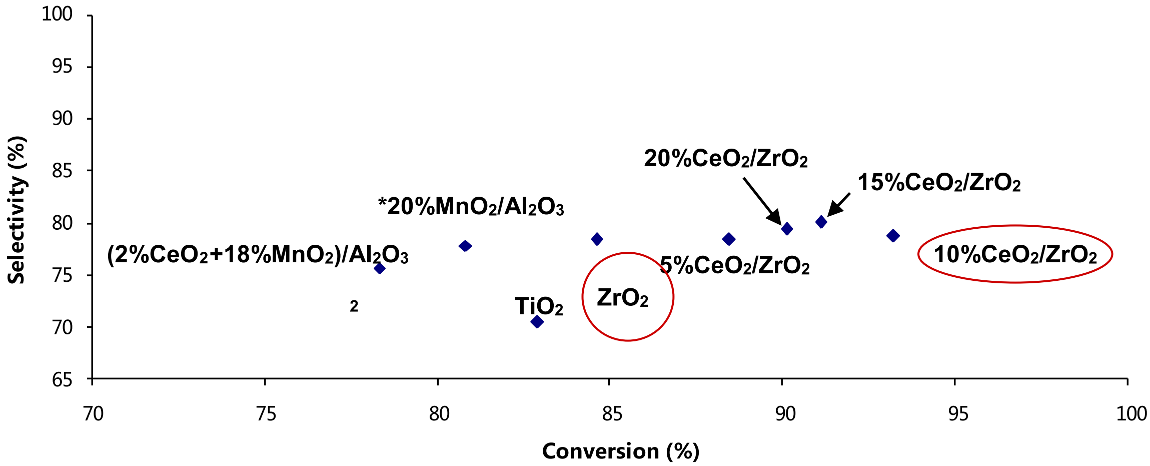

Fig. 11. Catalytic activity of metal oxides in ketonization of valeric acid. Reaction conditions (C_0 (VA) = 4.2 vol%, 628 K, PH_2 = 0.1 MPa, τ = 0.7 s, m_{cat} = 1 g) [93]. Reproduced with permission from Springer. *Activities of 20 wt% MnO_2/Al_2O_3 oxide catalysts are presented for comparison from [88].

liquid or gas phases on supported metal oxide catalysts. 5-nonanone was reported to be prepared from the concentrated solutions of levulinic acid by its multistage conversion into γ-valerolactone on Ru/C catalyst and then into VA and 5-nonanone over 1% Pd/Nb_2O_5 [37,87]. It was also found [37] that the transformation of VA into 5-nonanone can be carried out with sufficiently high selectivity on $Ce_{0.5}Zr_{0.5}O_2$ catalyst. Glinski and Kijenski performed ketonization of VA with high selectivity of 80%–94% in the gas phase on CeO_2/Al_2O_3 and MnO_2/Al_2O_3 oxide catalysts albert at low conversion [88].

An analysis of published data showed that systems based on ceria and zirconia are the most promising catalysts for the synthesis of ketones by the decarboxylation coupling of corresponding carboxylic acids. Different self-made mono- and bimetallic oxides (Al_2O_3, TiO_2, ZrO_2, CeO_2) were tested in the optimal reaction conditions (C_0 (VA) = 4.2 vol%, 628 K, PH_2 = 0.1 MPa, τ = 0.7 s) determined in the preliminary experiments (Fig. 10). The highest initial valeric acid conversion was observed over TiO_2 and ZrO_2 although titania deactivated fast with time-on-stream [89].

It has been checked also whether any binary catalytic systems containing two or three of these very active oxides show activity higher than the single oxide systems. Thus 5–20 wt% CeO_2/ZrO_2 [93], 10–20 wt% MnO_2/ZrO_2, 20 wt% MnO_2/Al_2O_3, 20 wt% CeO_2/Al_2O_3, 20 wt% (10%CeO_2 + 10%MnO_2)/Al_2O_3, 20 wt% (2%CeO_2 + 18%MnO_2)/Al_2O_3, 5–20 wt% CeO_2/TiO_2, 10 wt% MnO_2/TiO_2 were also tested under the same reaction conditions. The activity of all these metal oxides is presented in Fig. 11 in co-ordinates “selectivity-conversion” [93].

Among the tested catalysts the most interesting results were obtained for zirconia based catalysts (Fig. 11) [93,94]. Fig. 12 shows that VA conversion goes through the maximum achieved at 10% ceria in the mixed catalyst while selectivity was not dependent on CeO_2 content. Surprisingly addition of a only small amount of relatively inactive ceria resulted in a noticeable increase of zirconia activity. Contrary to that Gurbuz et al. observed intensification of 2-hexanone aldol condensation/hydrogenation using a dual catalyst bed in one reactor when ZrO_2 content increased, with neat ZrO_2 having the highest conversion of 90%. The main product for all catalysts is the primary condensation product, 7-methyl-5-undecanone. C_{12} products contained 5-methyl-undecane, resulting from deoxygenation of 7-methyl-5-undecanone [44]. A large number of surface acid sites for Pd/ZrO_2 is responsible for the

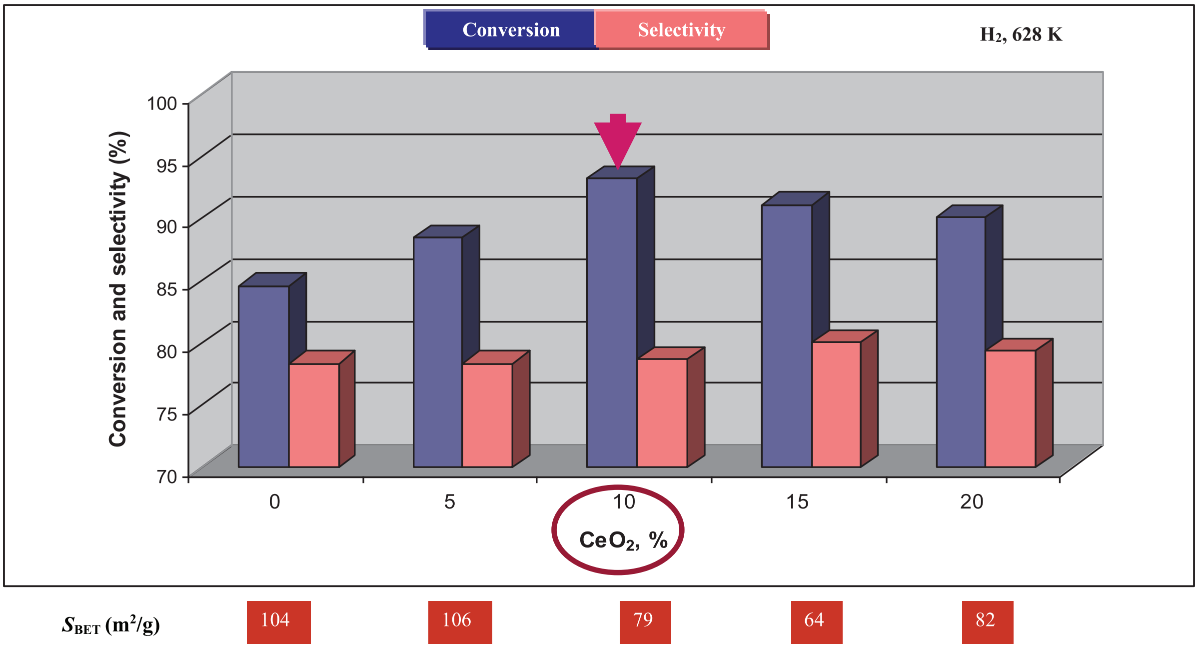

Fig. 12. Catalytic activity of zirconia modified with ceria metal oxides in ketonization of valeric acid. Reaction conditions (C_0 (VA) = 4.2 vol%, 628 K, $PH_2 = 0.1$ MPa, $\tau = 0.7$ s, $m_{cat} = 1$ g).

Table 1. C(VA) = 4.2 vol%, residence time = 0.7 s; $T = 628$ K; $P(H_2/N_2) \sim 0.1$ MPa [93]. Reproduced with permission from Springer.

Catalyst	Conversion (%)		Selectivity[a] (%)		S_{BET} (m^2/g)
	N_2	H_2	N_2	H_2	
CeO_2	31	40	80	76	25
ZrO_2	66	83	80	78	105
10%CeO_2/ZrO_2	82	93	81	79	79

[a] Selectivity was measured at the same conversion level.

increase in selectivity towards light alkanes, mainly hexane, as the dehydration of 2-hexanol to hexene as well as double bond shift or isomerization for C_9 ketones production is mainly catalyzed by acid sites. The increased activity of C–C hydrogenolysis to produce C_8 and C_{11} ketones on Pd/ZrO_2 may result from the absence of strong metal-support interactions (SMSI). In particular, it is known from the literature that ceria exhibits strong metal-support interactions [90], and the rate of C–C hydrogenolysis can be suppressed in the presence of SMSI [91]. Kunkes et al. have shown in [92] with temperature-programmed reduction (TPR) experiments that reduction of ceria occurs at these reduction temperatures, which is required for the onset of SMSI.

4.4. Effect of gas atmosphere

Traditionally ketonization reactions as well as aldol condensation are carried out under inert atmosphere. However, since the consecutive step of ketone transformation into alkane requires hydrogen, ketonization of VA was studied in presence of hydrogen [93]. The aim was to compare catalytic behavior under the reductive atmosphere vs. the inert one to understand which type of effect hydrogen atmosphere will provide on ketonization. 10 wt% CeO_2/ZrO_2 was found to demonstrate higher catalytic activity compared to zirconia *per se* as well as other ceria modified zirconia although ceria *per se* exhibited very low catalytic activity (Table 1).

Incorporation of ceria into ZrO_2 [93,94] was shown to result in an increase of catalytic activity due to (i) absence of an individual CeO_2 phase (which has low activity), (ii) formation of solid solution with intergrain boundaries in 10% CeO_2/ZrO_2 where ZrO_2 lattice structure is strongly disordered and exposes highly unsaturated coordination sites, and (iii) increase of total concentration of surface cations.

10 wt% CeO_2/ZrO_2 and ZrO_2 provided higher acid conversion in H_2 than in N_2 by 11%–17% whereas selectivity to 5-nonanone was rather insensitive to the gas atmosphere (Table 1) [93]. Hydrogen pretreatment was found to decrease adsorption sites acidity due to reduction $Zr^{4+} \rightarrow Zr^{3+}$ and $Ce^{4+} \rightarrow Ce^{3+}$ as well as to increase the amount of nucleophilic surface $O^{\delta-}$ species (XPS, FTIR, UV–vis) [94].

4.5. Mechanistic insight into ketonization

The changes of the catalyst surface cation composition affected the corresponding activity in ketonization. The origin of the changes is related to the reaction mechanism which involves metal cations catalytic sites (red circles) for carboxylate adsorption and stabilization as well as oxygen containing surface species (the lattice ions O^{2-} possessing nucleophilic properties) responsible for abstraction of proton from –COOH group and α-hydrogen (blue circles) (Fig. 13). The resulting carboxylate ions through participation of the surface hydroxyl groups, interact forming an intermediate compound, a β-ketoacid, which is then transformed to a ketone upon decarboxylation.

Pham et al. [95] reported that surface Ti^{3+} species similarly for TiO_2 can be readily formed and favor the acetic acid liquid phase ketonization when TiO_2/C was pre-reduced in situ with H_2. The resulting Ru/TiO_2/C catalyst exhibited higher activity and selectivity to acetone. When TiO_2/C sample was pre-calcined in air before addition of Ru, the resulting catalyst showed a significantly lower activity, even when it was pre-reduced in situ, and was essentially inactive without pre-reduction.

Carboxylate species can be adsorbed over surface metal cations in a number of different conformations during ketonization. A change in the binding type might play a significant role in determining the easiness with which the transition state is formed. There were numerous efforts reported in the literature aiming to

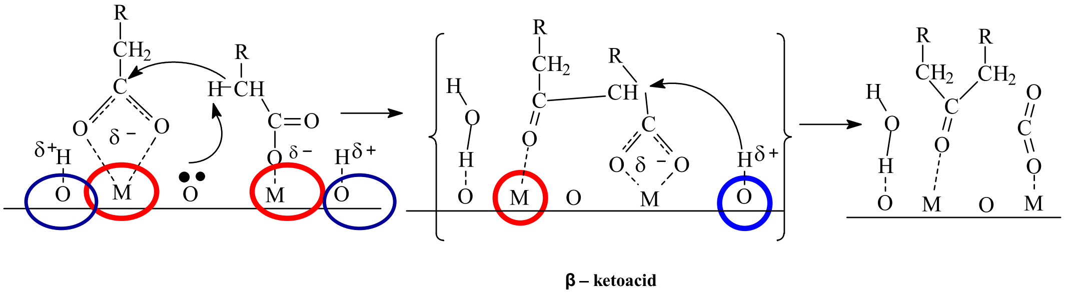

Fig. 13. Mechanism of carboxylic acid ketonization involving two types of active sites–metal cations and oxygen containing groups.

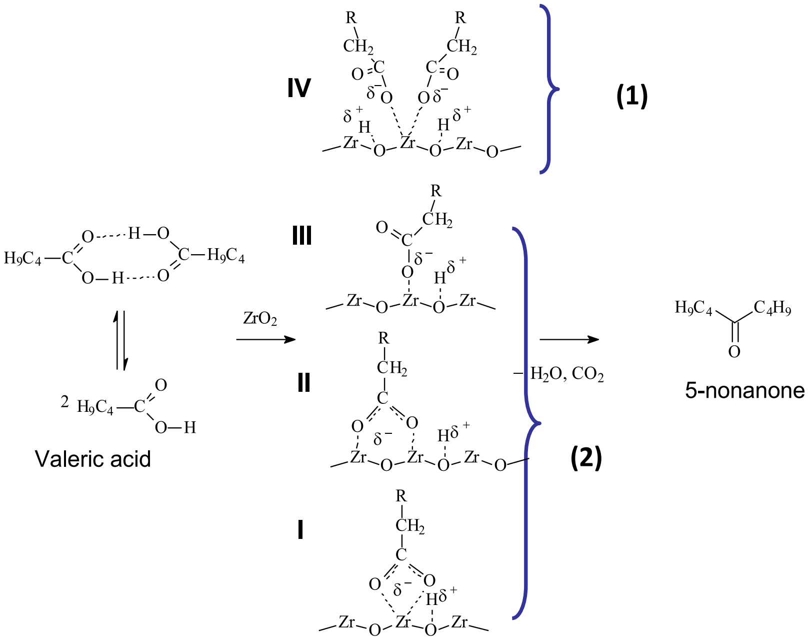

Fig. 14. Detailed mechanism of valeric acid ketonization with experimentally determined configurations of adsorbed valerates [99].

unravel possible configurations of carboxylate adsorption species using different approaches, e.g. interpreting DFT calculations for energy barriers in carboxylate formation on different crystal planes [84,96]. Pei and Ponec [97] corroborated carboxylates bidentates to be species of crucial importance, whereas Kim and Barteau [98] using TPD found that two acetate species should be monodentates coordinated to the same metal cation. Panchenko et al. examined adsorption of VA over ZrO_2 at room temperature directly by UV–vis and IR spectroscopy [99] and identified all chemisorption forms of VA on Lewis acid sites responsible for VA transformation: monomolecular (III) and bimolecular monodentate valerates (IV) (1740 cm^{-1}) as well as chelating (I) and bridging bidentate (II) valerates (1565 cm^{-1}) [99] (Fig. 14). When considering the valerate configurations which benefit mostly ketone formation, the probability of occurrence of one Zr LAS required for formation of e.g. structure (IV), is assumed to be much higher than the probability of an alternative case. The latter requires four zirconium LAS on ZrO_2 to be located within a distance needed for simultaneous landing of two acid molecules which eventually lead to formation of two structures (II). Thus, the mechanism involving one, two or even three Zr Lewis acid sites might be more preferred in this order of probability than the mechanism involving four Lewis acid sites located in close vicinity suggested, e.g. by Pulido et al. [84], even if the latter could in principle be a part of ketone formation mechanism. Based on the experimental data obtained by Panchenko et al. [99] and on DFT calculations reported in [96] a more detailed ketonization mechanism was proposed. It comprises two main pathways depending on the surface carboxylate intermediates: (1) via interactions of two monodentates coordinated to the same Zr cation (IV), and (2) via interactions of the surface chelating bidentate (I) with either monomolecular bridging bidentate (II) or monomolecular monodentate valerate (III). The relative contribution of each route to the overall ketone formation over metal oxide surfaces depends on the reaction conditions (Fig. 14).

4.6. *Ketonization kinetics*

The reaction rate of decarboxylative coupling in hydrogen over ZrO_2 was shown to have the second order on valeric acid [100] (Fig. 15) which is consistent with bimolecularity of the rate determining step assumed for the kinetically favored mechanism going through the β-ketoacid formation (Fig. 13). A similar second order was found for decarboxylative coupling of C_4, C_5 and C_6 acids in nitrogen under lower than 0.01 MPa hexanoic acid partial pressure whereas increasing the pressure above 0.01 MPa resulted in the zero order indicating a high acid coverage on the catalyst surface [101–103].

Apparent activation energy 60 ± 5 kJ/mol [100] for decarboxylative coupling over pre-reduced ZrO_2 in hydrogen atmosphere was found to be almost the same (60 ± 10 kJ/mol) as reported by Gaertner et al. for ketonization of C_5 acid into 5-nonanone over CeO_2-ZrO_2 in an inert gas [101]. Apparently the gas atmosphere does not affect the mechanism of decarboxylative

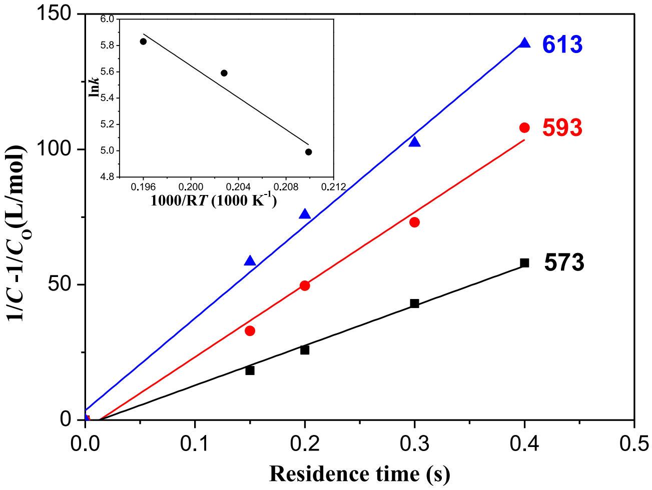

Fig. 15. Dependence of VA concentration on the residence time at 573, 593, 613 K. The inset shows the Arrhenius plot modified after [100]. Reaction conditions (C_0 (VA) = 4.2 vol%, $PH_2 = 0.1$ MPa, $m_{cat} = 1$ g).

coupling at low acid partial pressure while influencing active sites formation. Gaertner et al. [101] presented a kinetic model (1), that took into account both adsorption of the initial acid as well as carbon dioxide and water, while ketone adsorption was assumed negligible:

$$r = k \cdot P_{acid}^2 / (1 + K_{acid} \cdot P_{acid})^2 (1 + K_{H_2O} \cdot P_{H_2O} + K_{CO_2} \cdot P_{CO_2})^2 \qquad (1)$$

where r is the acid ketonization rate, k is the reaction constant, K_{acid}, K_{CO_2}, K_{H_2O}, P_{acid}, P_{CO_2}, P_{H_2O} are the adsorption constants and partial pressures of carboxylic acid, carbon dioxide and water, respectively. The model allows describing the transition in the reaction order dependence on the partial pressure of hexanoic acid from second to zero order with increasing acid concentration.

Note that the self-condensation products of 5-nonanone were not detected during valeric acid ketonization in hydrogen [100]. Similarly West et al. [104] did not observe the cross condensation between two ketone molecules which was assumed to be slower compared to the reaction of an aldehyde with a ketone and less thermodynamically favored [105]. Generally CO_2 produced in the ketonization reaction is a known poison for the basic sites active in aldol condensation [106,107]. Kunkes et al. reported [92] that the presence of 5% CO_2 in the feed is detrimental to aldol condensation activity (~90% decrease in activity) over Pd/$CeZrO_x$.

Noble metals supported on metal oxides were shown to have different activity in the liquid phase ketonic decarboxylation even changing reaction route [95,108]. Pham et al. showed that introduction of Ru into TiO_2 or TiO_2/C enhanced catalytic activity in acetic acid ketonization in *n*-hexane, *N*-methylpyrrolidone and water under N_2 after a preliminary catalyst reduction in-situ [95]. XPS, TPR, and EPR demonstrated that the incorporation of Ru resulted in the enhanced formation of Ti^{3+} sites. The hydrophobic activated carbon support also seems to help protecting the catalytic sites from water blockage and maintains activity in the aqueous phase.

5. Hydrodeoxygenation of ketone (5-nonanone) over Me/MeO_x

Second step in the preparation of oxygen-free alkanes from oxygenates involves hydrodeoxygenation of ketone functionality with an adequate reductive agent. Reduction of carbonyl group represents a quite complicate process in spite of its apparent simplicity.

5.1. Chemical reduction of ketones

The chemical reduction of ketones to methylene derivatives can be achieved by a number of reagents, the most prominent being zinc in combination with an acid as in the Clemmensen reduction, sodium borohydride with trifluoroacetic acid, as found by Gribble and coworkers, hydrazine with the base as in the Wolff–Kishner reduction, and combinations of $LiAlH_4$ and AlX_3 in diethyl ether [109]. Unfortunately, the most versatile of these reduction methods necessitates the use of strongly acidic or basic reagents with polar solvents, and such conditions can lead to undesired side reactions. Regarding catalytic asymmetric hydrogenation and transfer hydrogenation Wu and Xiao reported that asymmetric hydrogenation of simple alkyl ketones has been a difficult task because of the challenging differentiation of two similarly shaped sp^3-carbon groups connected to the carbonyl group. Up to now, the enantioselectivity still remains low and is generally lower than 80% ee [110].

5.2. Mechanistic view on catalytic reduction of ketones

A few works were found focusing on catalytic ketone hydrogenation not relevant to asymmetric catalysis. Kunkes et al. reported catalytic hydrogenation of an alkyl ketone proceeding first through hydrogenation to an alcohol with a subsequent dehydration to an olefin and final hydrogenation to an alkane [42]. Farkas and Farkas [111] have reported that in the vapor phase both acetone and isopropyl alcohol are converted to propane with either H_2 or D_2 over a platinum foil. From a relatively high rate of the reaction of acetone compared to alcohol, the authors concluded that the reduction to the hydrocarbon takes place directly from acetone rather than through the isopropyl alcohol as an intermediate. Further proof for the independence of the two reduction reactions was taken from experiments of Faillebien [111] who could show that in a liquid medium, using one type of catalyst, acetone or other ketones reacted with hydrogen to hydrocarbons, giving however alcohols with another type of catalysts. This was interpreted as occurrence of two independent reactions, each catalyzed by a separate catalyst. In addition Farkas et al. stated that the keto–enol reaction does not necessarily precede the formation of propane from acetone. Anderson et al. [112] postulated two mechanisms for converting a carbonyl group to an alcohol group using deuterium: (1) direct addition of D_2 to the carbonyl group $(CH_3)_2–C{=}O \rightarrow (CH_3)_2–CD–OD$, and (2) enolization of the carbonyl compound followed by addition of D_2 to the resulting ethylenic linkage $O{=}C(CH_3)–CH_3 \rightarrow OH–(CH_3)CH{=}CH_2 \rightarrow OH–CHD(CH_3)–CH_2D$. Chen and Chen also suggested that alcohols are not necessary intermediates for the production of alkanes from ketones [113]. The authors studied gas phase acetone hydrogenation on reduced and oxygen calcined (without reduction pretreatment) Pt/SiO_2 and Pd/SiO_2 catalysts and revealed that the propane formation rate increased with increasing the oxygen dosage on the catalyst contrary to isopropanol formation (~100% selectivity over fully reduced catalysts). The authors suggested that the mechanism of propane formation catalyzed by oxygen perturbed metal catalysts may be related to the formation of adsorbed acetone enolate species. The presence of the phenyl group facilitating enolization was shown to affect positively the methylene group formation providing a strong evidence for the above hypothesis [113]. Friedman and Turkevich conducted a deuterium exchange reaction accompanied by the reduction of acetone. It was found that the peak of the mass distribution of the polydeuteropropanes was 46 amu corresponding to $C_3H_6D_2$ structure [114]. This supported the above hypothesis being in line with the following reaction scheme (2):

$$CH_2{=}C(CH_3)–O_{(a)} \ldots HO_{(a)} + nD_2 \rightarrow C_3H_6D_2 + O_{(a)} + D_2O \qquad (2)$$

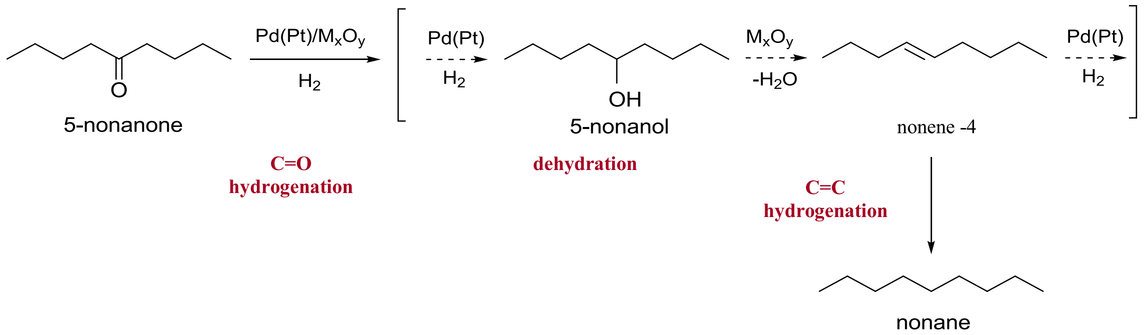

Fig. 16. The tentative scheme of 5-nonanone catalytic hydrogenation into *n*-nonane.

When combining ketone reduction to alcohol [112] with the final dehydration/hydrogenation step suggested by Kunkes et al. [42] the mechanism of ketone catalytic hydrogenation can be depicted in the following way:

(1) direct addition of D_2 to carbonyl group (to C=O bond):

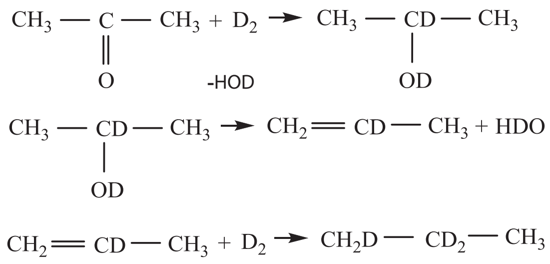

$$CH_3-\underset{\overset{\|}{O}}{C}-CH_3+D_2\rightarrow CH_3-\underset{\overset{|}{OD}}{CD}-CH_3$$
$$\text{-HOD}$$
$$CH_3-\underset{\overset{|}{OD}}{CD}-CH_3\rightarrow CH_2{=}CD-CH_3+HDO$$
$$CH_2{=}CD-CH_3+D_2\rightarrow CH_2D-CD_2-CH_3$$

(2) addition of D_2 to C=C double bond of enol form of carbonyl compound:

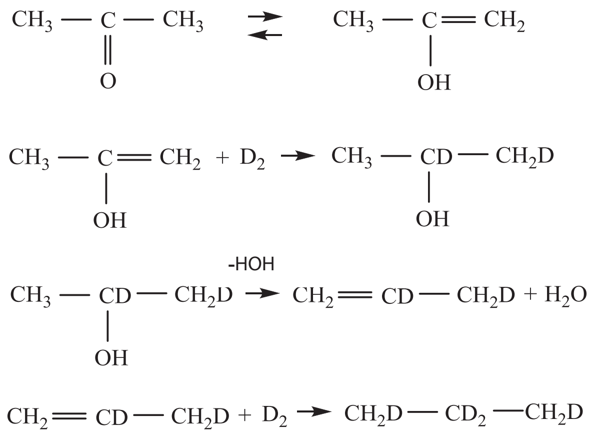

$$CH_3-\underset{\overset{\|}{O}}{C}-CH_3\rightleftarrows CH_3-\underset{\overset{|}{OH}}{C}{=}CH_2$$
$$CH_3-\underset{\overset{|}{OH}}{C}{=}CH_2+D_2\rightarrow CH_3-\underset{\overset{|}{OH}}{CD}-CH_2D$$
$$CH_3-\underset{\overset{|}{OH}}{CD}-CH_2D\xrightarrow{\text{-HOH}}CH_2{=}CD-CH_2D+H_2O$$
$$CH_2{=}CD-CH_2D+D_2\rightarrow CH_2D-CD_2-CH_2D$$

Bejblová et al. investigated catalytic hydrogenation and hydrogenolysis of acetophenone on Pd supported on active carbon, alumina and zeolites Beta and ZSM-5 in the liquid phase at temperatures 303–403 K and pressures 1–10 MPa. The kinetic model confirmed that the transformation of acetophenone to ethylbenzene proceeds primarily via a hydrogenation–dehydration mechanism and the effect of direct hydrogenolysis of the C=O bond of acetophenone is insignificant [115]. Török et al. suggested a mechanism of ketone hydrogenation over bifunctional Pt/K-10 catalyst where in the first step the carbonyl compound was reduced to the corresponding alcohol over Pt followed by dehydration over an acidic support and finally facile hydrogenation of alkene to the corresponding alkane on platinum surface [116]. Analyzing the individual steps, it was found that the rate (and yield) determining step is dehydration of the alcohol. C=O hydrogenation readily occurs at room temperature as well, similarly to the last step of C=C saturation. Dehydration, however, needs a relatively high temperature (433–443 K). The intermediate olefin was observed in hydrogen-free reaction [116].

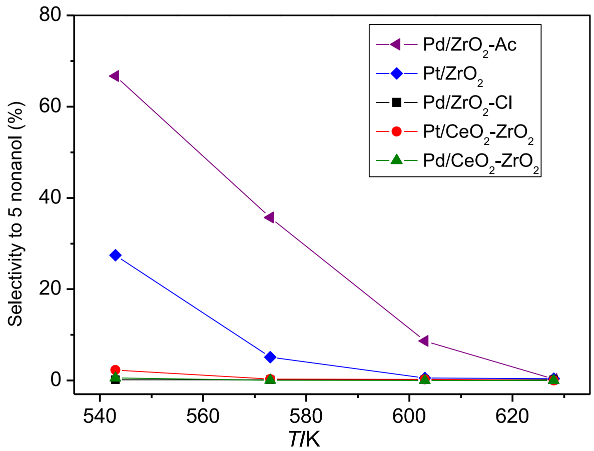

Fig. 17. Effects of temperature on selectivity to 5-nonanol in 5-nonanone hydrogenation. Reaction conditions: $T = 543$–628 K, $PH_2 \sim 0.6$ MPa, $\tau = 1.25$ s.

Accordingly Simonov et al. showed that catalytic hydrogenation of 5-nonanone proceeds through an intermediate formation of 5-nonanol followed by dehydration into 4-nonene (not observed) and hydrogenation to *n*-nonane [48]. The tentative scheme of catalytic hydrogenation of 5-nonanone is shown in Fig. 16.

5.3. Effect of the metal and support in ketone hydrogenation

The important question to be considered is related to the role of the hydrogenating metal and support in ketone reduction. Four Pd and Pt catalysts supported on the most active in ketonization metal oxides [93,94] were studied in 5-nonanone hydrogenation: Pd/ZrO_2, Pd/CeO_2-ZrO_2, Pt/ZrO_2, Pt/CeO_2-ZrO_2 [48,100]. Along with *n*-nonane 5-nonanol was observed in the course of the reaction. Selectivity to 5-nonanol was studied in the temperature range 543–628 K at 0.6 MPa hydrogen pressure (Fig. 17). It was found that formation of 5-nonanol was decreased with increasing temperature and was not observed in the presence Pd/ZrO_2, Pt/CeO_2-ZrO_2, Pd/CeO_2-ZrO_2 catalysts in all temperature interval. This could be a result of higher specific surface areas (96, 90, 88 m^2/g for Pd/ZrO_2, Pt/CeO_2-ZrO_2, Pd/CeO_2-ZrO_2, respectively) compared to Pd/ZrO_2-Ac and Pt/ZrO_2 (57 and 29 m^2/g, correspondingly) which apparently facilitated alcohol dehydration/hydrogenation preventing intermediate alcohol accumulation in the reaction mixture [48].

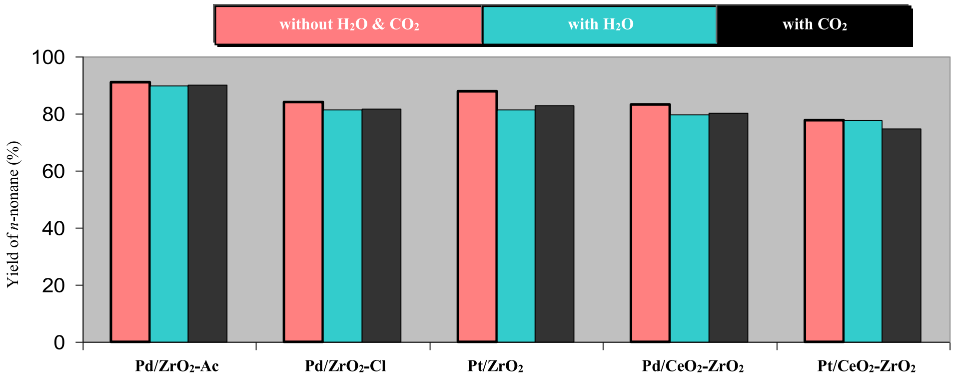

Fig. 18. Effect of CO_2 and H_2O on *n*-nonane yield in 5-nonanone hydrodeoxygenation over Pd/ZrO_2-Ac, Pd/ZrO_2-Cl, Pt/ZrO_2, Pd/CeO_2-ZrO_2, Pt/CeO_2-ZrO_2. $T = 628$ K, $PH_2 \sim 0.6$ MPa, residence time = 1.25 s, flow rates of CO_2 and/or H_2O 1.5 mL/min. Modified after [100].

Table 2. 2-Hexanone conversion and product distribution over 0.25 wt% Pd/CeO_x, Pd/$Ce_5Zr_2O_x$, Pd/$Ce_1Zr_1O_x$, Pd/$Ce_2Zr_5O_x$ and Pd/ZrO_2 with co-feeding 10 mol% CO_2 in H_2 stream at 623 K and 0.5 MPa, WHSV = 1.92 h^{-1} [43]. Reproduced with permission from Royal Society of Chemistry.

Catalyst	2-Hexanone conversion (%)	Selectivity to carbon (%)	
		C_{12}	C_{12+}
0.25 wt% Pd/CeO_x	4	34	0
0.25 wt% Pd/$Ce_5Zr_2O_x$	5	36	0
0.25 wt% Pd/$Ce_1Zr_1O_x$	5	22	0
0.25 wt% Pd/$Ce_2Zr_5O_x$	19	55	0
0.25 wt% Pd/ZrO_x	72	62	8

5.4. The effect of CO_2 and water in ketone reduction

To study the effect of CO_2 and water on the activity in 5-nonanone hydrogenation on Pd and Pt catalysts supported on ZrO_2 and 10% CeO_2-ZrO_2, carbon dioxide or water vapor were introduced into the reaction mixture fed to the catalyst bed at a constant flow in amounts comparable to the stoichiometric amounts generated in VA ketonization reaction. When the temperature was increased to 628 K no significant influence of carbon dioxide and water vapor was observed for all studied catalysts (Fig. 18) including Pt/CeO_2-ZrO_2, which is likely due to a more intense desorption of the introduced compounds at elevated temperatures diminishing potential inhibition of the vacant sites by these molecules. Pd/ZrO_2 showed higher activity and selectivity compared to Pd/CeO_2-ZrO_2 and Pt/ZrO_2, while better activity was observed for Pd/ZrO_2-Ac prepared from palladium acetate contrary to Pd/ZrO_2-Cl prepared from palladium chloride [100]. It is important to note that after the flow CO_2 or steam was stopped, the catalytic activity was completely restored.

A similar resistance of Pd/ZrO_2 catalyst to CO_2 and water poisoning in aldol condensation/hydrogenation was reported by Gurbuz et al. [44] whereas for ceria-containing catalysts such poisoning was dramatic. To explore the effect of CO_2 on aldol condensation/hydrogenation activity over the catalysts with different compositions, Gurbuz et al. [44] substituted neat hydrogen gas with H_2–CO_2 gas mixtures. All ceria-containing catalysts displayed a significant inhibition by CO_2, showing yields of less than 20% to C–C coupling products. The decrease in activity for these catalysts was found to correlate with the abundance of isolated O^{2-} sites which strongly bind CO_2, as shown in CO_2 TPD profiles. Pd/ZrO_2 showed a significant resistance to CO_2 poisoning (20% decrease in the condensation activity), since this catalyst did not contain strong CO_2 binding sites. The effect of CO_2 co-feeding on activity and selectivity to the condensation products is shown in Table 2 for all catalysts. Another by-product of ketonization, water, was shown to cause a decrease by 40% in the activity for aldol condensation of 2-butanone over Pd/$CeZrO_x$ when a mixture containing 12 wt% water in 2-butanone was used as the feed (Table 3) [92]. This inhibition by water is an additional obstacle for integration of ketonization and aldol condensation/hydrogenation steps. It has been shown in the literature that the nature of CO_2 interactions with the oxide surface can be modified by changing the composition of the mixed oxides [117,118].

5.5. Kinetic study of ketone reduction

Simonov et al. studied kinetics of vapor phase 5-nonanone hydrogenation into *n*-nonane in the presence of Pd/ZrO_2 [48]. To determine the rate constants and activation energy of 5-nonanone hydrogenation, the dependence of 5-nonanone concentration vs. the contact time at different reaction temperatures was investigated. It was found that the reaction rate has the first order in 5-nonanone. Activation energy of 5-nonanone hydrogenation was found to be 46 ± 5 kJ/mol. The order in hydrogen was calculated from the dependence of the reaction rate on hydrogen concentration in logarithmic coordinates, giving a values of 0.3 (Fig. 19).

Using a variety of supported platinum catalysts, Sen and Vannice [119] studied the metal-support effects in the liquid phase acetone hydrogenation between 303 and 333 K. Only one Langmuir–Hinshelwood model, with competitive adsorption of hydrogen and acetone and addition of the second hydrogen atom as the rate determining step provided a rate expression consistent with the experimental results. There is no general consensus on the mechanism of ketone hydrogenation because of different reaction conditions employed in different studies.

The discrepancy in the published results was attributed by some authors to differences in the catalyst composition [120]. A kinetic model was suggested also for hydrogenation of acetone, methyl ethyl ketone, methyl propyl ketone, and diethyl ketone [121].

The effects of the support on the reaction mechanism of acetophenone transformation over Pd catalysts supported on active carbon, alumina and zeolites Beta and ZSM-5 were studied by Bejblová et al. [115]. Catalysts with an acidic zeolite support showed a very high activity in the transformation of acetophenone to ethylbenzene. Acid properties of zeolites apparently procure water elimination from 1-phenylethan-1-ol as well as the consecutive formation of styrene. Another intermediate – methyl (1-phenylethyl) ether formed because of the acid properties of the zeolite via intermolecular dehydration of 1-phenylethan-1-ol with methanol. Nevertheless, styrene as a reaction intermediate was described even when an inert support like active carbon was used. In these systems, acid properties of the catalyst are due probably to palladium-activated hydrogen as it was described by, e.g., Červeny [122]. The

Table 3. 2-Butanone conversion and product distribution over Pd/ZrO_2 and $Pd/Ce_1Zr_1O_x$ in the presence and absence of water in the feed at 623 K and 0.5 MPa, WHSV = 1.92 h^{-1} [43]. Reproduced with permission from Royal Society of Chemistry.

Catalyst	Feed	2-Butanone conversion (%)	Carbon selectivity (%)	
			C_8	C_{8+}
0.25 wt% $Pd/Ce_1Zr_1O_x$	2-Butanone	69	91	5
0.25 wt% $Pd/Ce_1Zr_1O_x$	12 wt% water in 2-butanone	37	93	3
0.25 wt% Pd/ZrO_2	2-Butanone	88	77	11
0.25 wt% Pd/ZrO_2	12 wt% water in 2-butanone	78	80	9

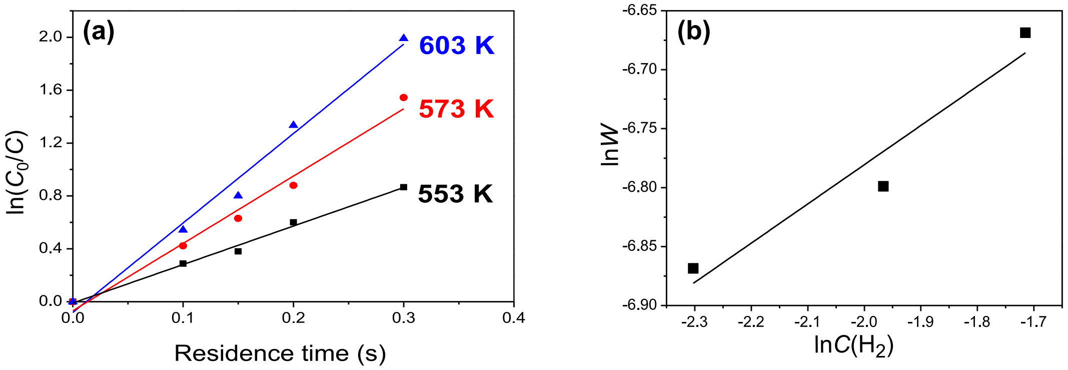

Fig. 19. Kinetics of 5-nonanone hydrogenation over Pd/ZrO_2. Reaction conditions: (a) 603 K, $PH_2 \sim 0.6$ MPa, $\tau = 0.25$ s, (b) 603 K, $PH_2 \sim 0.6$–1.0 MPa, $\tau = 0.25$ s. Modified after [48].

initial rates of acetophenone transformation are significantly influenced by the support acidity; namely the initial reaction rates increase with decreasing Si/Al ratio. On the other side, it is necessary to emphasize that the channel diameter of the zeolite used obviously does not play a key role in the reaction rate. For both ZSM-5 (with channel size of 0.53–0.55 nm) and Beta (large-pore zeolite, 0.76–0.64 nm) zeolites the initial rates of acetophenone transformation were similar being dependent more on the concentration of aluminum than on the channel size of a particular zeolite [115]. MCM-41 along with alumina and active carbon were considered as less appropriate supports for benzophenone hydrodeoxygenation than zeolites due to their low acidity [123].

Li et al. [124] investigated hydrodeoxygenation of difurfurylidene acetone dimer (F_2A) to liquid alkanes (C_8–C_{14}) at 533 K in a batch reactor over 1 wt% Pt catalysts supported on SAPO-11, HZSM-5, SiO_2-Al_2O_3, MCM-22, and self-synthesized SiO_2-ZrO_2. Moderately high C_8–C_{14} alkanes yield of ca. 56% was obtained over the optimized 1 wt% Pt/SiO_2-ZrO_2 catalyst which can be attributed to moderate acidic centers and a proper pore size of 9.0 nm. In addition more than 10% of oxygenated hydrocarbons, including C_{11}–C_{13} chain alcohols and ketones and the hydrogenated F_2A dimers with furan ring were obtained. In order to improve the liquid alkane yield, a two-step process for F_2A conversion was also investigated, which included low-temperature hydrogenation at 323 K over Raney Ni catalyst in a batch reactor and the subsequent high-temperature hydrodeoxygenation at 553 K over 1 wt% Pt/SiO_2-ZrO_2 in a fixed-bed reactor.

5.6. Solvent effects in ketone reduction

The course of liquid phase ketone hydrogenation can be also affected by the solvent as it was shown for acetophenone hydrogenation [125,126]. The solvent effect has been observed in the liquid-phase hydrogenation by many authors (for example, Iwamoto et al. [127], Lemcoff [128]). Kishida and Teranishi [129] reported that nonpolar solvents (saturated hydrocarbons) promoted acetone hydrogenation over different nickel catalysts at room temperature, while polar solvents (primary alcohols and amines) inhibited the reaction. These observations imply that polar solvent molecules compete with ketone for the active sites. Bejblová et al. [115] showed that the effect of the solvent (polar methanol and nonpolar hexane) on the initial rate of acetophenone transformation, r_0, (Fig. 20) as well as on the selectivity of 1-phenylethan-1-ol production (Fig. 21) is not straightforward [115].

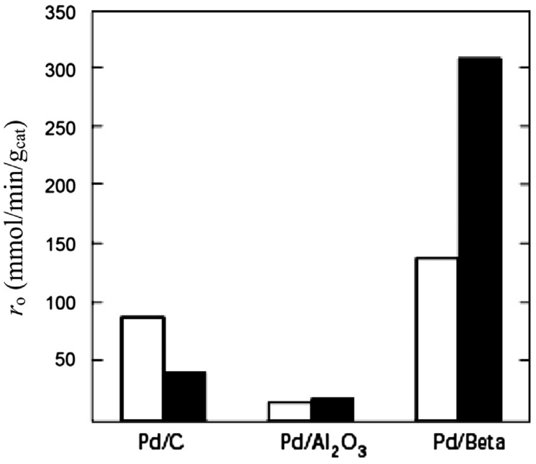

Fig. 20. Effect of the solvent (☐ methanol, ■ hexane) on the initial reaction rate of acetophenone hydrogenation r_0 [115]. Copyright 2003 Institute of Organic Chemistry and Biochemistry.

With Pd/C catalyst the initial rate in methanol was twice as high as in hexane. On the contrary, for Pd/Al_2O_3 the initial rates did not significantly differ in the case of Pd/zeolite catalysts (e.g., zeolite Beta), the rate was significantly higher in hexane. These results imply that the acidity of different supports obviously affects the initial rate of acetophenone decomposition depending on the type of the solvent used. On acidic zeolites polar methanol competitively adsorbs together with acetophenone, whereas in hexane as a solvent acetophenone is preferentially adsorbed. Selectivity to 1-phenylethan-1-ol at 50% acetophenone conversion was slightly higher in hexane with all types of catalysts. The most apparent effect of the solvent was observed with 5 wt% Pd/Al_2O_3. In methanol, the final product of acetophenone

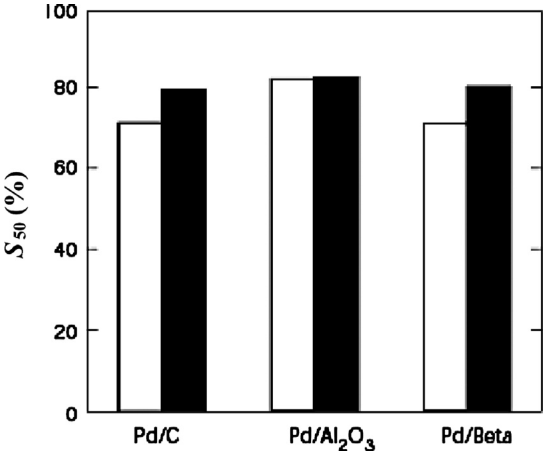

Fig. 21. Effect of the solvent (☐ methanol, ■ hexane) on the selectivity to 1-phenylethan-1-ol at 50% acetophenone conversion [115]. Copyright 2003 Institute of Organic Chemistry and Biochemistry.

hydrogenation led to 1-phenylethan-1-ol (selectivity ca. 75%), which was not further hydrogenated under the reaction conditions. This unambiguously demonstrated that the catalyst deactivation was present. On the other hand, when hexane was used as a solvent under the same reaction conditions, 1-phenylethan-1-ol reacted further as an intermediate resulting in 65% of ethylbenzene and 23% of 1-phenylethan-1-ol. Contrary to that Bejblová et al. reported a higher initial rate of benzophenone hydrodeoxygenation observed in the presence of Pd catalysts supported on active carbon, alumina, zeolites Beta and ZSM-5 and MCM-41 with methanol as a solvent compared to hexane [123].

McManus et al. [130] studied the effect of solvent on the competitive hydrogenation of 4-phenyl-2-butanone over Pt/TiO$_2$ and Pt/SiO$_2$ in *n*-hexane, toluene, *tert*-butyl toluene, 1-propanol, 2-propanol and dibutyl ether. For the titania catalyst, alkanes were found to favor ring hydrogenation whereas aromatics and alcohols led to carbonyl hydrogenation. A two-site catalyst model was proposed whereby the aromatic ring hydrogenation occurs over the metal sites while carbonyl hydrogenation is thought to occur predominantly at interfacial sites, with oxygen vacancies in the titania support activating the carbonyl. The effect of the solvent on the hydrogenation reaction over the titania catalyst was related to competition for the active sites between solvent and 4-phenyl-2-butanone.

5.7. Effect of ketone structure

Török et al. [116] studied catalytic hydrogenation by a bifunctional 5% Pt/K-10 catalyst with a variety of ketones of different structures. It was found that the aliphatic ketones react faster than the cyclic compounds, with C$_6$ ring-containing derivatives reacting especially slow requiring long reaction time to obtain good yields. For some reactants with a specific structure the product formed did not correspond to the expected one. Pinacolone and camphor, undergoing readily the reduction formed rearranged products according to Wagner–Meerwein rearrangement with the driving force being formation of more stable carbocations. Diketones can be also reduced, e.g. *n*-hexane is formed from acetonylacetone with 98% yield [116].

Kong et al. studied efficient hydrodeoxygenation of aliphatic ketones over an alkali-treated Ni/HZSM-5 catalyst in a fixed-bed reactor [131]. The experimental results indicated that alkali-treated Ni/HZSM-5 exhibited excellent performance for this reaction. Alkaline treatment sharply reduced the amount of strong acid sites on the catalyst and also generated a large number of mesopores in the catalyst. The decrease of strong acid sites suppresses the formation of low-boiling products and aldol-condensation side products, while the mesopores improved hydrogenation and dehydration performances of the catalyst. These two aspects also promoted the catalyst excellent time-on-stream performance. Additionally, the generality of the alkali-treated Ni/HZSM-5 was proved in that work as most of the selected carbonyl compounds could be hydrodeoxygenated to the corresponding alkanes with selectivity exceeding 97.0 %.

5.8. Effect of the metal size in ketone hydrogenation

The size effect on activity and selectivity in ketone hydrogenation was scarcely reported in the literature. Analysis of 5-nonanone conversion in the presence of Pd/ZrO$_2$ with average Pd particle sizes 1.1, 1.7, 2.1 and 2.9 nm at 543 K indicates a strong dependence of the catalytic activity of Pd particle size. However, catalytic activity based on the amount of available surface metal atoms is practically independent on the size of the metal particles [48]. These data are in a good agreement with the classical concepts of structure insensitivity of hydrogenation reactions [132,133], and are experimentally confirmed in a study of the size effect in ketone hydrogenation. Thus, in hydrogenation of 1-phenyl-1,2-propanedione in the presence of Pt/Al$_2$O$_3$ a weak dependence of the reaction rate on the metal dispersion was found, while enantioselectivity and regioselectivity were largely changed [134]. Structure insensitivity was established in enantioselective hydrogenation of ethyl pyruvate on Pt nanoparticles [135]. Similar structure insensitive behavior was found for hydrogenation of the double bond in 2-cyclohexenone in the presence of Rh/SiO$_2$ [136]. At the same time for some carbonyl compounds the structure sensitivity was reported. For example in methyl isobutyl ketone hydrogenation to 2-methylpentane over 0.5% Pt/HZSM [137] or cyclohexenone hydrogenation in the presence of colloidal platinum particles [138] activity increased with increasing metal dispersion. Apparently, the presence of various functional groups as well as the presence of a sterically bulk substituent have a substantial effect on the reactivity of the substrates, making establishing a general correlation between activity and the metal dispersion in hydrogenation of the carbonyl group of various compounds difficult. In crotonaldehyde hydrogenation the overall turnover frequency (TOF) and selectivity to crotyl alcohol (related to selective hydrogenation of C=O functionality) increased with increasing particle size [139,140,141]. Grass et al. studied dependence of the gas-phase crotonaldehyde hydrogenation selectivity and activity on the size of Pt nanoparticles (1.7–7.1 nm) supported on SBA-15 [142] and found threefold role of the particle size. The first is related to the fraction of exposed atoms in close packed (111) planes vs. those at coordinatively unsaturated sites or in open faces such as (100) or (110). Larger nanoparticles have a larger fraction of atoms in terraces with a close packed structure than smaller particles and are selective for the formation of crotyl alcohol. The second reason for the particle size dependent selectivity is the steric hindrance of the C=C bond, which is more easily accommodated on smaller nanoparticles. Catalytic activity is also lower over such nanoparticles because decarbonylation of crotonaldehyde to CO and C$_3$ hydrocarbons as well as other C–C bond breaking reactions occur preferentially on the corner and edge sites which are more predominant at higher metal dispersion [143].

6. One-pot process

One of the strategies of the carboxylic acids transformations considered in the literature suggests their direct conversion into alkanes in a one-pot mode. One-pot or tandem catalytic transformations in a single reactor possess significant challenges as the conditions for all individual transformations could be different,

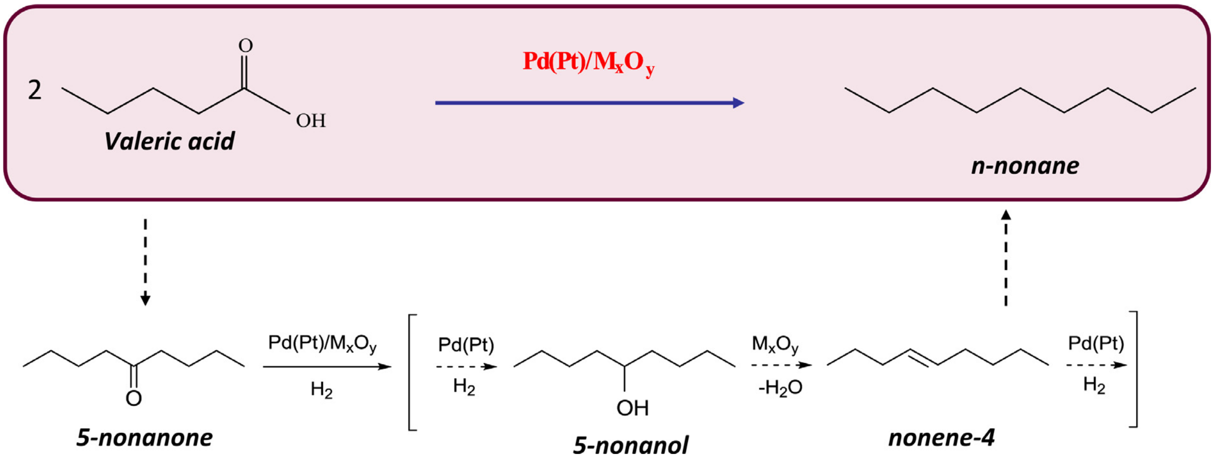

Fig. 22. Scheme of one-pot vapor phase transformation of valeric acid into *n*-nonane.

moreover there could be interactions between the catalytic species and the active sites of a particular catalyst, which are not necessarily beneficial. The rate of the processes should be harmonized, otherwise one type of catalysis could be for instance substrate starved thus diminishing the benefits of the multiple operation. One-pot carboxylic acid conversions have been reported in the literature involving combinations of ketonization/hydrodeoxygenation in a single or a double catalyst beds as well as ketonization and aldol condensation/hydrogenation in double-bed catalysts.

There is certain confusion in the literature with respect to terminology of one-pot/tandem or domino/cascade-type processes. Domino/cascade mode of operation refers to processes where the intermediate cannot be isolated and the individual steps cannot be performed separately. Contrary to it conventional reactions performed sequentially are referred as tandem reactions, being also able to provide significant process improvements, when performed in an one-pot fashion.

Integration of ketonization and aldol condensation/hydrogenation reactions in a single reactor, double-bed system was suggested by Gurbuz et al. [43]. The results of that study involving different compositions of ceria-zirconia mixed-oxide catalysts indicated that Pd/ZrO_2 is the preferred catalyst to be used for integration of ketonization and aldol condensation/hydrogenation reactions in a single reactor system. Pd/ZrO_2 has high activity being resistant to inhibition by CO_2 and water. To test the applicability of a double-bed system, a 20 mol% mixture of butanoic acid in 2-hexanone was used as the feed (Table 4). These results demonstrated that Pd/ZrO_2 is resistant to CO_2 and water generated in the ketonization step for this simulated feed mixture.

Based on the previously found regularities of VA ketonization in the presence of ZrO_2 in hydrogen atmosphere [93] and hydrodeoxygenation of 5-nonanone in the presence of CO_2 and H_2O (Fig. 18) Pd/ZrO_2-Ac, Pd/CeO_2-ZrO_2, Pt/CeO_2-ZrO_2 catalysts were studied in one-pot transformation of valeric acid into *n*-nonane (Fig. 22) at 543–628 K, hydrogen pressure of 0.6–1.0 MPa and residence time 0.36–1.45 s.

Among these catalysts Pd/ZrO_2 was chosen as the best one for carrying out the one-pot process being the most stable compared to Pd/CeO_2-ZrO_2 and Pt/CeO_2-ZrO_2 (Fig. 23).

Investigation of the activity of a bifunctional catalyst Pd/ZrO_2 in cascade-type VA reaction in the temperature range 543–628 K showed that the highest activity of the catalyst was achieved at 628 K. By increasing the hydrogen pressure from 0.6 to 1.0 MPa at a constant temperature 628 K a slight gradual increase in the yield of *n*-nonane from 80 to 90% was observed. A comparison of two modes for VA conversion into *n*-nonane under optimized reaction conditions demonstrated that the one-pot process provides a higher *n*-nonane yield (81%) compared to that in a consecutive two stage process (65%) indicating a noticeable advantage of the one-pot process affording formation of alkanes potentially suitable for diesel fuel.

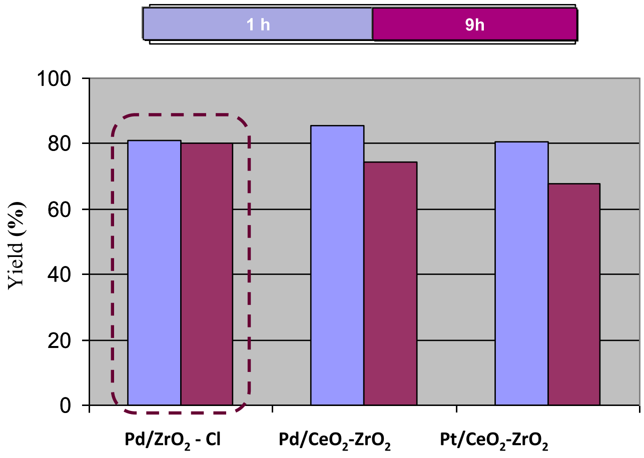

Fig. 23. *n*-Nonane yield in 1 or 9 h in one-pot vapor phase VA transformation over Pd/ZrO_2-Cl, Pd/CeO_2-ZrO_2, Pt/CeO_2-ZrO_2. Reaction conditions: $T = 628$ K, $PH_2 \sim 0.6$ MPa, $\tau = 1.45$ s. Modified after [100].

Corma et al. [3] also showed that zirconia is a very selective and stable catalyst in obtaining hydrocarbons of the kerosene range from hexose-derived VA. This oxide when combined with platinum supported on alumina diminished the oxygen content to almost zero (Fig. 24).

Furthermore, the authors demonstrated that alumina is superior to active carbon, silica, or zirconia as a support for the hydrogenation/dehydration/hydrogenation sequence and a palladium-based catalyst deactivated more rapidly than the platinum catalyst. As a result of that study under optimized reaction conditions VA was converted into *n*-nonane with 80% selectivity (together with 10% of C_{10}–C_{15} hydrocarbons) in the organic liquid phase at up to 100:1 feed to catalyst ratio (w/w). The oxygen free hydrocarbon product mixture (85% yield) complies well with the boiling point range of kerosene as evidenced by a simulated distillation (Fig. 25). In the gas phase, butane was detected together with mainly carbon dioxide.

Table 4. 2-Hexanone and butanoic acid conversions and product selectivity for reaction of 2-hexanone containing 20 mol% butanoic acid or 20 mol% heptane over the double-bed system at 623 K and 0.5 MPa [43]. Reproduced with permission from Royal Society of Chemistry.

Feed (balance 2-hexanone)	Conversion (%)		Carbon selectivity (%)						
	2-Hexanone	Butanoic acid	4-Heptanone	C_{12}	C_{15}	C_{18+}	C_9	C_8 and C_{11}	Alkanes ($<C_7$)
20 mol% heptane	76	–	–	51	5	11	9	5	19
20 mol% butanoic acid	75	100	11	45	5	5	12	7	14

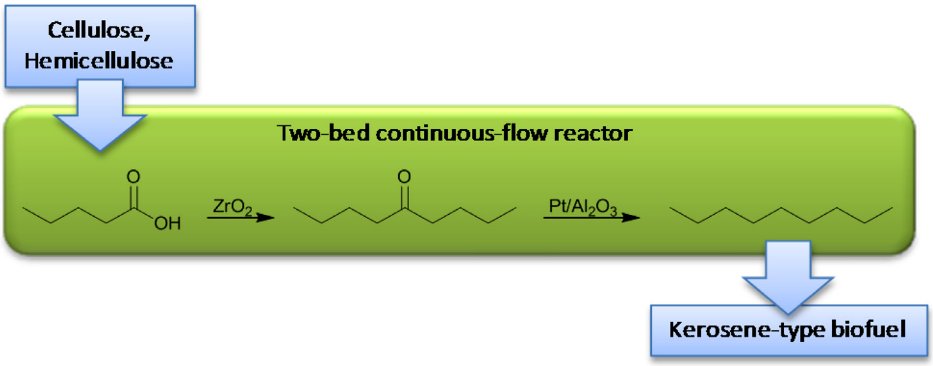

Fig. 24. Scheme of two-bed continuous synthesis *n*-nonane from valeric acid [3]. Reproduced with permission.

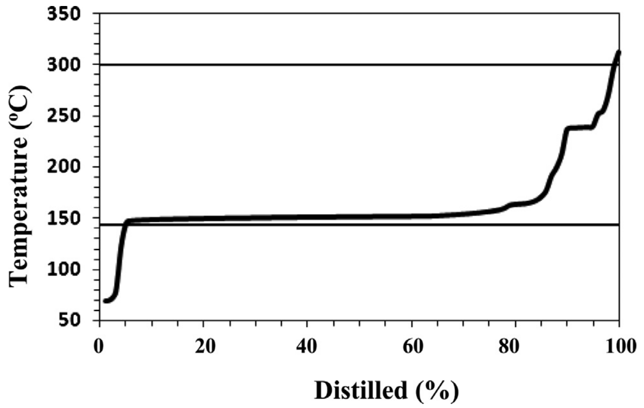

Fig. 25. Simulated distillation for the product mixture obtained when VA was passed over a ZrO_2 and a Pt/Al_2O_3 bed having as a basis kerosene boiling point range from 418 to 573 K [3]. Reproduced with permission.

7. Conclusions

Carboxylic acids play a prevailing role in biomass transformations into fuels and chemicals when lignocellulose is considered as a feedstock. They are presented widely in plant oils, tall oil, and can be formed as bio-oil components through pyrolysis of lignocellulosic biomass. Carboxylic acids, such as levulinic acid, are easily available via hydrolysis of hexoses as in the Biofine process. Valeric acid can be formed from levulinic acid with >80% yield opening up new way for synthesis of fuels and chemicals. For both type of desired products, fuels and chemicals, the reduction of the oxygen content lowering the acidity, as well as an increase of the alkyl chain length decreasing volatility is an important issue. Ketonic decarboxylation matches perfectly these requirements as it converts carboxylic acids into ketones forming one carbon–carbon bond eliminating three oxygen atoms as carbon dioxide and water. Zirconia and ceria modified zirconia were shown to be the most active and selective catalysts of carboxylic acid ketonization among different metal oxides investigated in the literature. Ketonization reaction rate depends on Lewis sites acidity which in turn is dependent on catalyst surface reduction. Reductive atmosphere favors formation of more basic Me^{3+} from Me^{4+}, decreasing acidity of adsorption sites and enhancing acid adsorption. In addition such atmosphere increases the amount of nucleophilic surface $O^{\delta-}$ species, benefiting abstraction of α-H^+ from adsorbed acid species. Acid conversion in optimal conditions provides ca. 80% of the ketone yield. Different chemisorption forms of valeric acid on Lewis acid sites were found: monomolecular and bimolecular monodentate valerates as well as chelating and bridging bidentate valerates that could be a part of the reaction mechanism occurring through the β-ketoacid formation. Catalytic reduction of ketone over Pd or Pt supported catalysts proceeding through formation of an intermediate alcohol followed by dehydration into alkene and hydrogenation to alkane requires presence of acidic and hydrogenation sites in a catalyst with a high surface area. Effect of the cluster size of the hydrogenation metal requires further clarification although structure insensitivity of the reaction was clearly shown for a narrow Pd particle size range 1.7–2.9 nm over Pd/ZrO_2. Pd/ZrO_2 demonstrated the highest resistance to CO_2 and water as well as selectivity to alkane. Different approaches were suggested for the one-pot alkane production from VA. The combination of ZrO_2 with Pt/Al_2O_3 placed in this order in a fixed-bed continuous flow reactor provided excellent stability with time on stream yielding ca. 80% of *n*-nonane. Multifunctional properties of Pd/ZrO_2 also allow an excellent combination of ketonic decarboxylation with hydrodeoxygenation in a single bed on the one-pot reactor. The one-pot process requires a presence of basic sites for carboxylic acid binding during the ketonization step as well as acidic sites for alcohol dehydration along with hydrogenation sites for the ketone hydrodeoxygenation step. Obviously ZrO_2 is the preferred support for Pd or Pt bearing catalysts in the one-pot process having an adequate combination of acidic and basic sites as well as developed surface area for effective catalytic performance. A comparison of two modes for VA conversion into *n*-nonane under optimized reaction conditions over Pd/ZrO_2 demonstrated that the one-pot process exhibits a higher *n*-nonane yield (81%) compared to a consecutive two stage process (65%). These results indicate a noticeable advantage of the one-pot process affording formation of alkanes potentially suitable for diesel fuel. The presence of hydrogenation metal at the beginning of the ketonization step seems to enhance promoting interactions of hydrogen with the metal oxide surface ions, thereby accelerating ketonization.

Acknowledgments

This work was partly supported by Russian Academy of Science Project No. V.46.4.4. Part of work related to metal oxides was supported by RFBR grant 15-03-09329.

References

[1] J.C. Serrano-Ruiz, D.J. Braden, R.M. West, J.A. Dumesic, Appl. Catal. B: Environ. 100 (2010) 184–189.
[2] J.C. Serrano-Ruiz, R.M. West, J.A. Dumesic, Annu. Rev. Chem. Biomol. Eng. 1 (2010) 79–100.
[3] A. Corma, B. Oliver-Tomas, M. Renz, I.L. Simakova, J. Mol. Catal. A: Chem. 388–389 (2014) 116–122.
[4] J.P. Lange, ChemSusChem 2 (2009) 587–592.
[5] V. Dornburg, B.G. Hermann, M.K. Patel, Environ. Sci. Technol. 42 (7) (2008) 2261–2267.
[6] P. Gallezot, Chem. Soc. Rev. 41 (4) (2012) 1538–1558.
[7] V.F. Tret'yakov, Yu.I. Makarfi, K.V. Tret'yakov, N.A. Frantsuzova, R.M. Talyshinskii, Catal. Ind. 2 (2010) 402–420.
[8] J.C. Serrano-Ruiz, J.A. Dumesic, Green Chem. 11 (2009) 1101–1104.
[9] D.M. Alonso, J.Q. Bond, J.A. Dumesic, Green Chem. 12 (2010) 1493–1513.
[10] N. Arun, R.V. Sharma, A.K. Dalai, Renew. Sustain. Energy Rev. 48 (2015) 240–255.
[11] K. Yan, Y. Yang, J. Chai, Y. Lu, Appl. Catal. B: Environ. 179 (2015) 292–304.
[12] M. Patel, X. Zhang, A. Kumar, Renew. Sustain. Energy Rev. 53 (2016) 1486–1489.
[13] Y. Zhang, P. Bi, J. Wang, P. Jiang, X. Wu, H. Xue, J. Liu, X. Zhou, Q. Li, Appl. Energy 150 (2015) 128–137.
[14] Md.I. Alam, B. Saha, Sustainable Catalytic Processes, Elsevier, Amsterdam, 2015, pp. 99–123.
[15] S. De, B. Saha, R. Luque, Bioresour. Technol. 178 (2015) 108–118.
[16] D. Ghosh, D. Dasgupta, D. Agrawal, S. Kaul, D.K. Adhikari, A.K. Kurmi, P.K. Arya, D. Bangwal, M.S. Negi, Energy Fuels 29 (2015) 3149–3157.
[17] Y. Liu, L. Chen, T. Wang, Q. Zhang, C. Wang, J. Yan, L. Ma, ACS Sustain. Chem. Eng. 3 (2015) 1745–1755.
[18] P. Maki-Arvela, B. Holmbom, T. Salmi, D.Y. Murzin, Catal. Rev. Sci. Eng. 49 (2007) 197–340.
[19] Y. Pu, D. Zhang, P.M. Singh, A.J. Ragauskas, Biofuels Bioprod. Biorefin. 2 (2008) 58–73.
[20] I. Delidovich, K. Leonhard, R. Palkovits, Energy Environ. Sci. 7 (2014) 2803–2830.
[21] M. Snåre, P. Mäki-Arvela, I.L. Simakova, J. Myllyoja, D.Yu. Murzin, J. Phys. Chem. B 3 (2009) 17.
[22] D.Yu. Murzin, I.L. Simakova, Catal. Ind. 3 (3) (2011) 218–249.
[23] P. Mäki-Arvela, I.L. Simakova, T. Salmi, D.Yu. Murzin, Chem. Rev. 114 (3) (2014) 1909–1971.
[24] M.N. Simonov, I.L. Simakova, V.N. Parmon, React. Kinet. Catal. Lett. 97 (1) (2009) 157–162.
[25] T. Werpy, G. Petersen, Top Value Added Chemicals from Biomass, vol. 2, US Department of Energy DOE/GO-102004-1992, August 2004, http://www.eere.energy.gov/biomass/pdfs/35523.pdf.
[26] J.J. Bozell, L. Moens, D.C. Elliott, Y. Wang, G.G. Neuenscwander, S.W. Fitzpatrick, R.J. Bilski, J.L. Jarnefeld, Resour. Conserv. Recycl. 28 (2000) 227–239.
[27] J.J. Thomas, R.G. Barile, Energy Biomass Wastes 8 (1984) 1461–1494.
[28] M. Kitano, F. Tanimoto, M. Okabayashi, Chem. Econ. Eng. Rev. 7 (1975) 25–29.
[29] S.W. Fitzpatrick, World Patent 9640609, 1997.
[30] R.O.M.A. de Souza, L.S.M. Miranda, R. Luque, Green Chem. 16 (2014) 2386–2405.
[31] K. Kon, W. Onodera, K.-I. Shimizu, Catal. Sci. Technol. 4 (2014) 3227–3234.
[32] W. Luo, P.C.A. Bruijnincx, B.M. Weckhuysen, J. Catal. 320 (2014) 33–41.
[33] X. Tang, X. Zeng, Z. Li, L. Hu, Y. Sun, S. Liu, T. Lei, L. Lin, Renew. Sustain. Energy Rev. 40 (2014) 608–620.
[34] L. Deng, Y. Zhao, J. Li, Y. Fu, B. Liao, Q.X. Guo, ChemSusChem 3 (2010) 1172–1175.
[35] F.M.A. Geilen, B. Engendahl, A. Harward, W. Marquardt, J. Klankermayer, W. Leitner, Angew. Chem. 49 (2010) 5510–5514.
[36] K. Hengst, M. Schubert, H.W.P. Carvalho, C. Lu, W. Kleist, J.-D. Grunwaldt, Appl. Catal. A: Gen. 502 (2015) 18–26.
[37] J.C. Serrano-Ruiz, D. Wang, J.A. Dumesic, Green Chem. 12 (2010) 574–577.
[38] P.M. Ayoub, J.P. Lange, WO 2008/142 127, 2008.
[39] W.F. Maier, W. Roth, I. Thies, P. Rague-Schleyer, Chem. Ber. 115 (1982) 808–812.
[40] A. Corma, M. Renz, C. Schaverien, ChemSusChem 1 (2008) 739–741.
[41] Y.M. Chung, O.Y. Kim, H.J. Jeon, Y.S. Yoon, S.H. Lee, H.S. Kim, S.H. Oh, Y.J. Yim, US Patent 2013017590, 2013.
[42] E.L. Kunkes, D.A. Simonetti, R.M. West, J.C. Serrano-Ruiz, C.A. Gärtner, J.A. Dumesic, Science 322 (2008) 417–421.
[43] E.I. Gurbuz, E.L. Kunkes, J.A. Dumesic, Green Chem. 12 (2010) 223–227.
[44] E.I. Gurbuz, E.L. Kunkes, J.A. Dumesic, Appl. Catal. B: Environ. 94 (2010) 134–141.
[45] S.G. Wettstein, D.M. Alonso, E. Gurbuz, J.A. Dumesic, Curr. Opin. Chem. Eng. 1 (2012) 218–224.
[46] S. Murat Sen, E.I. Gurbuz, S.G. Wettstein, D.M. Alonso, J.A. Dumesic, C.T. Maravelias, Green Chem. 14 (2012) 3289–3294.
[47] O.O. Ayodele, F.A. Dawodu, D. Yan, X. Lu, J. Xin, S. Zhang, Renew. Energy 86 (2016) 943–948.
[48] M.N. Simonov, Yu.A. Gulaeva, I.P. Prosvirin, I.A. Chetyrin, I.L. Simakova, J. Sib. Fed. Univ.: Chem. 4 (2013) 331–343.
[49] I.V. Deliy, I.L. Simakova, N. Ravasio, R. Psaro, Appl. Catal. A: Gen. 357 (2) (2009) 170–177.
[50] D.Yu. Murzin, I.L. Simakova, Comprehensive Inorganic Chemistry II: From Elements to Applications, second ed., Elsevier, Amsterdam, 2013, p. 559.
[51] R. Rinaldi, F. Schüth, Energy Environ. Sci. 2 (2009) 610–626.
[52] O. Nagashima, S. Sato, R. Takahashi, T. Sodesawa, J. Mol. Catal. 227 (2005) 231–239.
[53] P. Pestman, R.M. Koster, A. van Duijne, J.A.Z. Pieterse, V. Ponec, J. Catal. 168 (1997) 265–272.
[54] R.P. Eischens, Science 146 (1964) 486–493.
[55] M. Glinski, G. Zalewski, E. Burno, A. Jerzak, Appl. Catal. A: Gen. 470 (2014) 278–284.
[56] M. Glinski, J. Kijenski, A. Jakubowski, Appl. Catal. A: Gen. 128 (1995) 209–217.
[57] K. Parida, H.K. Mishra, J. Mol. Catal. A: Chem. 139 (1999) 73–80.
[58] Y. Lee, J.-W. Choia, D.J. Suh, J.-M. Ha, C.-H. Lee, Appl. Catal. A: Gen. 506 (2015) 288–293.
[59] J.C. Serrano-Ruiz, J.A. Dumesic, ChemSusChem 2 (2009) 581–586.
[60] A. Westfechtel, C. Breucker, B. Gutsche, L. Jeromin, H. Eierdanz, H. Baumann, K.H. Schmid, W. Nonnenkamp, Patent DE 4121117, 1993.
[61] A. Leung, D.G.B. Boocock, S.K. Konar, Energy Fuels 9 (1995) 913–920.
[62] N. Saito, Patent JP 08198796, 1996.
[63] V.I. Yakerson, A.M. Rubinshtein, L.A. Gorskaya, Patent GB 1208802, 1970.
[64] J. Graille, D. Pioch, Patent EP 457665, 1991.
[65] D. Pioch, R. Lescure, J. Graille, Corps. Gras. Lipides 2 (1995) 386–389.
[66] E. Mueller-Erlwein, B. Rosenberger, Chem. Ing. Tech. 62 (1990) 512–513.
[67] M. Renz, Eur. J. Org. Chem. (2005) 979–988.
[68] G. Vavon, A. Apchie, Bull. Soc. Chim. 43 (1928) 667–677.
[69] J.F. Thorpe, G.A.R. Kon, Org. Synth. Coll. 1 (1941) 192–194.
[70] W. Klein-Homann, Patent DE 3709765, 1988.
[71] J. Stubenrauch, E. Brisha, J.M. Vohs, Catal. Today 28 (1996) 431–441.
[72] R. Novothy, S. Paulsen, Patent DE 1158050, 1963.
[73] T.S. Hendren, K.M. Dooley, Catal. Today 85 (2003) 333–351.
[74] R. Martinez, M.C. Huff, M.A. Barteau, J. Catal. 222 (2004) 404–409.
[75] K. Matsuoka, K. Tagawa, Patent JP 61207354, 1985.
[76] Daicel Chem Ind., Patent JP 57197237, 1982.
[77] J.C. Kuriacose, R. Swaminathan, J. Catal. 14 (1969) 348–354.
[78] R. Swaminathan, J.C. Kuriacose, J. Catal. 16 (1970) 357–362.
[79] J. Cressely, D. Farkhani, A. Deluzarche, A. Kiennemann, Mater. Chem. Phys. 11 (1984) 413–431.
[80] J.C. Kuriacose, S.S. Jewur, J. Catal. 50 (1977) 330–341.
[81] M. Renz, A. Corma, Eur. J. Org. Chem. (2004) 2036–2039.
[82] A.A. Taimoor, A. Favre-Reguillon, L. Vanoye, I. Pitault, Catal. Sci. Technol. 2 (2012) 359–363.
[83] S. Rajadurai, Catal. Rev. Sci. Eng. 36 (1994) 385–403.
[84] A. Pulido, B. Oliver-Tomas, M. Renz, M. Boronat, A. Corma, ChemSusChem 6 (2013) 141–151.
[85] O. Neunhoeffer, P. Paschke, Chem. Ber. 72 (1939) 919–929.
[86] H. Kwart, K. King, The Chemistry of Carboxylic Acids and Esters, Interscience, New York, 1969.
[87] A.D. Patel, J.C. Serrano-Ruiz, J.A. Dumesic, R.P. Anex, Chem. Eng. J. 160 (2010) 311–321.
[88] M. Glinski, J. Kijenski, React. Kinet. Catal. Lett. 69 (2000) 123–128.
[89] I.L. Simakova, V.N. Panchenko, Y. Gulyaeva, M. Simonov, XIIth European Congress on Catalysis (EuropaCat-XII), Kazan, August 30–September 4, 2015, pp. 79–80.
[90] M. Abid, V. Paul-Boncour, R. Touroude, Appl. Catal. A 297 (2006) 48–59.
[91] S.A. Stevenson, G.B. Raupp, J.A. Dumesic, S.J. Tauster, R.T.K. Baker. In: S.A. Stevenson, J.A. Dumesic, R.T.K. Baker, E. Ruckenstein eds. MetalSupport Interactions in Catalysis, Sintering, and Redispersion. New York: Van Nostrand Reinhold Company, 1987. pp. 55–75.
[92] E.L. Kunkes, E.I. Gurbuz, J.A. Dumesic, J. Catal. 206 (2009) 236–249.
[93] Yu.A. Zaytseva, V.N. Panchenko, M.N. Simonov, A.A. Shutilov, G.N. Zenkovets, I.L. Simakova, V.N. Parmon, Top. Catal. 56 (2013) 846–855.
[94] A.A. Shutilov, M.N. Simonov, Yu.A. Zaytseva, G.A. Zenkovets, I.L. Simakova, Kinet. Catal. 54 (2) (2013) 184–192.
[95] T.N. Pham, D. Shi, T. Sooknoi, D.E. Resasco, J. Catal. 295 (2012) 169–178.
[96] C. Hammaecher, J.-F. Paul, J. Catal. 300 (2013) 174–182.
[97] Z.-F. Pei, V. Ponec, Appl. Surf. Sci. 103 (1996) 171–182.
[98] K.S. Kim, M.A. Barteau, J. Catal. 12 (1990) 353–375.
[99] V.N. Panchenko, Yu.A. Zaytseva, M.N. Simonov, I.L. Simakova, E.A. Paukshtis, J. Mol. Catal. A: Chem. 388–389 (2014) 133–140.
[100] Yu.A. Gulyiaeva, Study of valeric acid catalytic conversion into alkanes in consecutive reactions of ketonization and hydrogenation for synthesis of fuel components PhD Thesis, Novosibirsk, Russia, 2014 http://rue.catalysis.ru/Public/Avref/Gulaeva.pdf.
[101] C.A. Gaertner, J.C. Serrano-Ruiz, D.J. Braden, J.A. Dumesic, Ind. Eng. Chem. Res. 49 (2010) 6027–6033.
[102] R.W. Snell, B.H. Shanks, ACS Catal. 3 (2013) 783–789.
[103] D. Todd, J. Am. Chem. Soc. 71 (1949) 1353–1355.

[104] R.M. West, Z. Liu, M. Peter, J.A. Dumesic, ChemSusChem 1 (2008) 417–424.
[105] E.L. Kunkes, D.A. Simonetti, R.M. West, J.C. Serrano-Ruiz, C.A. Gaertner, J.A. Dumesic, Science 322 (2008) 417–421.
[106] S. Abello, D.V. Shankar, J. Perez-Ramirez, Appl. Catal. A: Gen. 342 (2008) 119–125.
[107] Y. Kamimura, S. Sato, R. Takahashi, T. Sodesawa, T. Akashi, Appl. Catal. A: Gen. 252 (2003) 399–410.
[108] Y.K. Lugo-José, J.R. Monnier, C.T. Williams, Appl. Catal. A: Gen. 469 (2014) 410–418.
[109] J.J. Eisch, Z.-R. Liu, M.P. Boleslawski, J. Org. Chem. 57 (1992) 2143–2141.
[110] X. Wu, J. Xiao, in: P. Knochel, G.A. Molander (Ed.), Comprehensive Organic Synthesis II, vol. 8, Elsevier, 2014, p. 198.
[111] A. Farkas, L. Farkas, J. Am. Chem. Soc. 61 (1939) 1336–1341.
[112] L.C. Anderson, N.W. MacNaughton, J. Am. Chem. Soc. 64 (1942) 1456–1459.
[113] H.-W. Chen, C.-S. Chen, Catal. Lett. 39 (1996) 39–41.
[114] L. Friedman, J. Turkevich, J. Am. Chem. Soc. 74 (1952) 1669–1671.
[115] M. Bejblová, P. Zamostny, L. Červeny, J. Čejka, Collect. Czech. Chem. Commun. 68 (2003) 1969–1984.
[116] B. Török, G. London, M. Bartók, Synlett Issue 5 (2000) 631–632.
[117] J.I. DiCosimo, V.K. Diez, M. Xu, E. Iglesia, C.R. Apesteguia, J. Catal. 178 (1998) 499–510.
[118] V.K. Diez, J.I. DiCosimo, C.R. Apesteguia, Appl. Catal. A 345 (2008) 143–151.
[119] B. Sen, M.A. Vannice, J. Catal. 113 (1988) 521–571.
[120] P. Fouilloux, G.A. Martin, A.J. Renouprez, B. Moraweck, B. Imelik, M. Prettre, J. Catal. 25 (1972) 212–222.
[121] N.-S. Chang, S. Aldrett, M.T. Holtzapple, R.R. Davison, Chem. Eng. Sci. 55 (2000) 5721–5732.
[122] L. Červeny, Chem. Eng. Commun. 83 (1989) 31–35.
[123] M. Bejblova, P. Zamostny, L. Cerveny, J. Cejka, Appl. Catal. A: Gen. 296 (2005) 169–175.
[124] Y. Li, X. Huang, Q. Zhang, L. Chen, X. Zhang, T. Wang, L. Ma, Appl. Energy 162 (2016) xxx.
[125] E.C. Horning, D.B. Reisner, J. Am. Chem. Soc. 71 (1949) 1036–1037.
[126] L. Červeny, V. Růžička, Sb. Vys. Sk. Chem. Technol. Praze, C 27 (1981) 61–67.
[127] L.O. Iwamoto, T. Anouma, T. Keii, Int. Chem. Eng. 11 (1971) 573–577.
[128] N.O. Lemcoff, J. Catal. 46 (1977) 356–364.
[129] S. Kishida, S. Teranishi, J. Catal. 12 (1968) 90–96.
[130] I. McManus, H. Daly, J.M. Thompson, E. Connor, C. Hardacre, S.K. Wilkinson, N. Sedaie Bonab, J. ten Damc, M.J.H. Simmons, E.H. Stitt, C. D'Agostino, J. McGregor, L.F. Gladden, J.J. Delgado, J. Catal. 330 (2015) 344–353.
[131] X. Kong, W. Lai, J. Tian, Y. Li, X. Yan, L. Chen, ChemCatChem 5 (2013) 2009–2014.
[132] M. Che, C.O. Bennett, Adv. Catal. 36 (1989) 55–172.
[133] G.C. Bond, Surface Sci. 156 (1985) 966–981.
[134] D.Yu. Murzin, E. Toukoniitty, React. Kinet. Catal. Lett. 90 (2007) 19–25.
[135] E. Schmidt, A. Vargas, T. Mallat, A. Baiker, J. Am. Chem. Soc. 131 (2009) 12358–12367.
[136] E. Ronzo, G. Del Angel, J. Mol. Catal. A: Chem. 148 (1999) 105–115.
[137] M.A. Alotaibi, E.F. Kozhevnikova, I.V. Kozhevnikov, Chem. Commun. 48 (2012) 7194–7196.
[138] N.E. Musselwhite, S.B. Wagner, K.A. Manbeck, A. Kimberly, L.M. Carl, K.M. Gross, A.L. Marsh, L. Anderson, Appl. Catal. A: Gen. 402 (2011) 104–109.
[139] G.F. Santori, M.L. Casella, G.J. Siri, H.R. Aduriz, O.A. Ferretti, React. Kinet. Catal. Lett. 75 (2002) 225–230.
[140] A. Giroir-Fendler, D. Richard, P. Gallezot, Catal. Lett. 5 (1990) 175–181.
[141] M. Englisch, A. Jentys, J.A. Lercher, J. Catal. 166 (1997) 25–35.
[142] M.E. Grass, R.M. Rioux, G.A. Somorjai, Catal. Lett. 128 (2009) 1–8.
[143] I.L. Simakova, O.A. Simakova, P. Mäki-Arvela, A.V. Simakov, M. Estrada, D.Yu. Murzin, Appl. Catal. A: Gen. 355 (1–2) (2009) 100–108.